follows (only the one strand is shown). LOX1-GC; 5'-GAATTTGC GTCAGCGAACTTCTT, ACO-DR1; 5'-GAACGTGACCTTTGTC CTGGT which is corresponding to the PPRE for the rat acyl-CoA oxidase gene. In some experiments, nuclear extracts were preincubated with excess amount of unlabeled oligonucleotides, 1 μg of goat control IgG, or 1 μg of a goat anti-PPARα polyclonal antibody (Santa Cruz Biotechnology) at room temperature for 30 min. These mixtures were subjected to electrophoresis through 5% (wt/vol) polyacrylamide gels containing 10% glycerol. The dried gels were analyzed by Fuji Bioimage Analyzer BAS2400 (Fuji Photo Film).

Statistical analysis. Statistical significance in differences between groups was determined by one factor analysis of variance with Fisher PLSD as post hoc test, and statistical significance between two groups was determined by Student's *t* test. A value of $p < 0.05$ was considered significant.

Results

LOX-1 expression is upregulated by PPARα ligands but not by PPARγ ligands in cultured bovine aortic endothelial cells

After confluent monolayers of bovine aortic endothelial cells (BAECs) were treated with or without various PPARα ligands, such as fenofibrate and WY14643, as well as PPARγ ligands, such as troglitazone and 15-deoxy-$\Delta^{12,14}$-prostaglandin J_2 (15d-PGJ_2), for 12 h, total cell lysates and total cellular RNA were isolated and subjected to immunoblot and Northern blot analyses, respectively. As shown in Fig. 1A, the bar graph, indicating semi-quantification of LOX-1 protein expression, shows that PPARα ligands, such as fenofibrate (100 μM) or WY14643 (250 μM), prominently induced LOX-1 protein expression. In contrast, PPARγ ligands, such as troglitazone (15 μM) or 15d-PGJ_2 (3 μM), did not significantly affect LOX-1 protein expression. Fig. 1B demonstrates that LOX-1 mRNA was remarkably induced by fenofibrate and WY14643 (PPARα ligands), but not by 15d-PGJ_2 or troglitazone (PPARγ ligands), as shown by Northern blotting. Treatment with various concentrations of fenofibrate (0–200 μM) showed that LOX-1 protein expression was upregulated in a dose-dependent manner (Fig. 2A). Time-course experiments showed that increased LOX-1 protein expression was found as early as 3 h after the addition of fenofibrate, peaked after 24 h, and sustained for 48 h (Fig. 2B).

PPARα ligands increased the uptake of DiI-labeled oxidized LDL which was not inhibited by excess amounts of unlabeled acetylated LDL

To determine whether upregulated expression of LOX-1 by PPARα ligands is correlated with enhanced uptake of oxidized LDL (Ox-LDL), amounts of DiI-labeled Ox-LDL internalized into BAECs were measured. Because LOX-1 can take up Ox-LDL but not Ac-LDL, we measured the amounts of DiI-labeled Ox-LDL taken

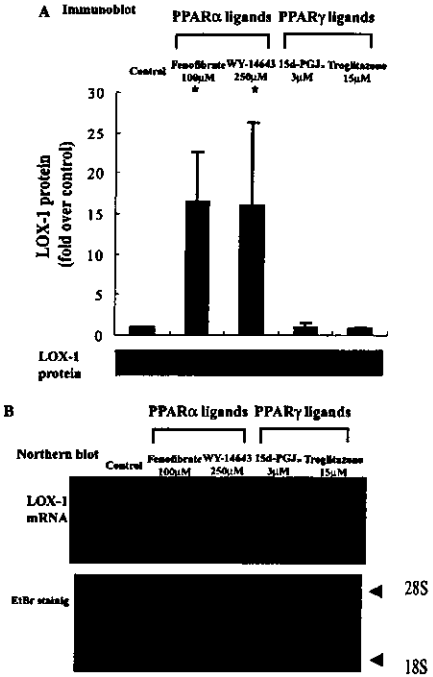

Fig. 1. Induction of LOX-1 expression by PPARα ligands in BAECs. (A) Immunoblot analyses for LOX-1 in BAECs treated with various PPAR ligands. Cells were treated with or without (control) the indicated concentrations of PPAR ligands for 16 h and subjected to immunoblot analyses. A bar graph indicates semi-quantification analysis from three independent experiments. Mean values and the standard deviations are indicated. LOX-1 protein induced by fenofibrate or WY14643 was significantly increased, compared to control ($p < 0.05$). There are no significant differences between that of fenofibrate and WY 14643. A representative figure of immunoblotting is also shown. (B) Northern blot analyses for LOX-1 mRNA in BAECs treated with various PPAR ligands. BAECs were treated with or without (control) the indicated concentrations of PPAR ligands for 16 h and subjected to Northern blot analyses. Each lane contained 15 μg of total RNA. A representative figure is shown from three independent experiments. Lower panel shows ethidium bromide staining of the RNA gel.

up by Ox-LDL- specific pathways that cannot be inhibited by excess amounts of unlabeled Ac-LDL. After treatment with or without PPAR ligands for 12 h, BAECs were incubated with DiI-labeled Ox-LDL in combination with the 100-fold excess amounts of unlabeled Ac-LDL for additional 2 h. PPARα ligands, but not a PPARγ ligand troglitazone, increased the internalization of DiI-Ox-LDL, as shown in Fig. 3A.

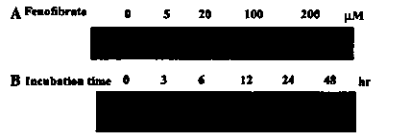

Fig. 2. Dose–response relationship (A) and time-course (B) of LOX-1 protein expression induced by a PPARα ligand, fenofibrate. (A) BAECs were treated with the indicated concentrations of fenofibrate for 12 h, and subjected to immunoblot analyses. (B) BAECs were treated with 100 μM of fenofibrate for the indicated time periods and subjected to immunoblot analyses.

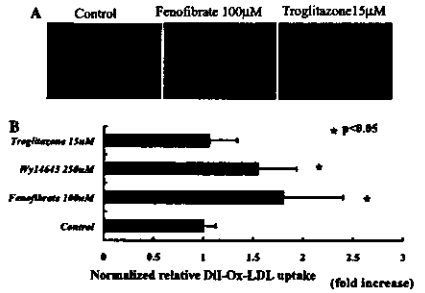

Fig. 3. PPARα ligands increased the specific uptake of Ox-LDL which is distinct from acetylated LDL uptake. After treatment with the indicated reagents for 12 h, BAECs were incubated with 5 μg/ml of DiI-labeled Ox-LDL in combination with 500 μg/ml of unlabeled Ac-LDL for an additional 2 h. (A) Fluorescence microscopic pictures are shown. (B) Quantitative analyses of DiI-labeled Ox-LDL uptake in BAECs treated with the indicated reagents. Columns indicate the mean of relative fluorescence intensities normalized against cellular protein concentrations from six wells. Bars represent standard deviations.

Quantification of the DiI-Ox-LDL uptake in BAECs showed that PPARα ligands enhanced Ox-LDL specific uptake by approximately 2-fold, but troglitazone did not (Fig. 3B). These results demonstrated that increases in LOX-1 expression by PPARα ligands were associated with enhanced Ox-LDL-specific uptake in BAECs.

Inhibition of PPARα expression by antisense oligonucleotides suppressed fenofibrate- induced LOX-1 expression

To confirm that fenofibrate-induced LOX-1 expression depends upon PPARα, effects of antisense ODNs against PPARα were examined. Transfection of antisense ODNs directed to PPARα significantly suppressed PPARα mRNA expression as expected. In contrast, neither sense, missense nor scrambled ODNs suppressed PPARα expression. PPARα/GAPDH mRNA ratios were as follows; antisense: 0.13 ± 0.03, sense: 0.55 ± 0.06 missense: 0.27 ± 0.10, and scrambled: 0.43 ± 0.07 ($p < 0.05$: antisense vs. sense, missense or scrambled; Fig. 4A). As shown in Fig. 4B, reduced expression of PPARα resulted in suppressed LOX-1 expression induced by fenofibrate. Transfection of sense, missense, or scrambled, ODNs against PPARα did not significantly reduce fenofibrate-induced LOX-1 expression (antisense: 2.2 ± 0.6-fold, sense: 6.7 ± 0.7-fold missense: 6.2 ± 1.3-fold, and scrambled: 6.1 ± 1.5-fold increases compared with untreated control, $p < 0.05$: antisense vs. sense, missense or scrambled; Fig. 4B).

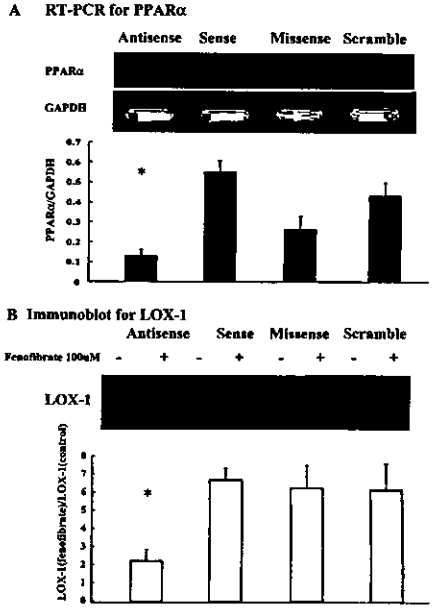

Fig. 4. Effects of antisense oligonucleotides (sODN) for PPAR α on fenofibrate-induced expression of LOX-1 BAECs were transfected with 10 μM of the indicated sODN by use of Lipofectamine 2000. After 24 h incubation, these cells were incubated with or without fenofibrate for additional 16 h, and then subjected to RT-PCR for PPARα (A) and immunoblotting for LOX-1 (B). (A) Antisense sODN for PPARα significantly suppressed PPAR α mRNA expression. Total RNA isolated from BAECs was subjected to RT-PCR. Upper panel shows the representative figure. Lower panel shows quantification of PPARα/GAPDH mRNA ratio. (*$p < 0.05$ compared with sense, missense, or scrambled sODN). (B) Increased expression of LOX-1 was blocked by antisense sODN. Upper panel shows a representative figure of immunoblotting for LOX-1. Lower panel indicates a bar graph showing semi-quantification of LOX-1 expression by fenofibrate. Mean values and the standard deviations calculated from 5-wells are indicated. (*$p < 0.05$ compared with sense, missense, or scrambled sODN).

GC box motif at −114/−106 region of the LOX-1 gene promoter is responsible for PPARα-induced transcription of LOX-1 gene

We have further analyzed transcriptional regulation of LOX-1 gene by PPARα. Schematic illustration of the luciferase-reporter constructs used in this study, containing various lengths of 5′ flanking region of human LOX-1 gene with or without mutated GC box, is shown in Fig. 5A. All these constructs contained TPA-responsive element (TRE) at −60/−53. At 24 h after transfection with the indicated promoter–reporter gene constructs, BAECs were incubated with or without fenofibrate (100 μM) or WY14643 (250 μM) for additional 12 h, and then luciferase activities were measured. promoter–reporter gene constructs containing −167/+31 region, including GC box, showed significant increases, which is comparable with those containing −3141/+31 or −2423/+31, in the luciferase activity by fenofibrate or WY14643; however, a point mutation in the GC box (PGL3-p2423M and PGL3-p167M) did not show statistically significant increases by fenofibrate or WY14643 (asterisks; Fig. 5B). In contrast, both promoter–reporter constructs containing wild-type and mutated GC box motif (PGL3-p167 and PGL3-167M) responded well to phorbol 12-myristate 13-acetate (PMA) stimulation (Fig. 5B), indicating that this GC box is not necessary for PMA-induced LOX-1 gene transcription but TPA-responsive elements (TRE) at −60/−53 might be involved. These results thus indicate that the GC box motif located in −167/+31 region of the LOX-1 gene is a specific *cis*-element for PPARα-induced transcription of LOX-1 gene.

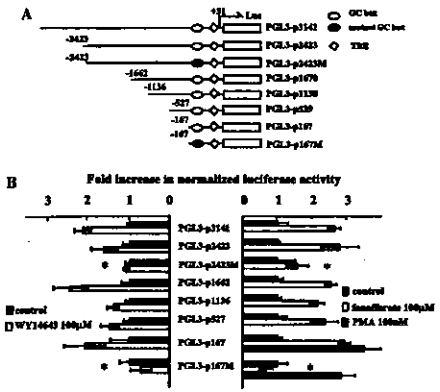

Fig. 5. Identification of a *cis*-acting element responsible for LOX-1 gene transcription by PPARα ligands. (A) Scheme of LOX-1 promoter-luciferase gene constructs containing various lengths of 5′ flanking region of the LOX-1 gene with or without the mutated GC box. (B) BAECs were transfected with the indicated promoter–reporter gene constructs. After 24 h incubation, these cells were incubated with or without fenofibrate (100 μM), WY14643 (250 μM), or phorbol 12-myristate 13-acetate (PMA; 100 nM) for additional 12 h, and then luciferase activities were measured. Fold increases compared to mean values of the controls after normalization by an internal transfection control (pRL-TK) are indicated. Data are means ± standard deviations from five samples for each experimental condition. Asterisks (*) indicate that significant increases in luciferase activities by fenofibrate or WY14643 were abrogated.

Activated PPARα binds to the GC box motif in the promoter region of LOX-1 gene.

To determine whether activated PPARα by fenofibrate in nuclei can bind to the GC box motif in the promoter region of human LOX-1 gene, an electrophoretic mobility shift assay (EMSA) was performed using nuclear extract from BAECs incubated with or without fenofibrate, using the GC box motif oligonucleotides (LOX1-GC) or the oligonucleotides corresponding to PPRE for acyl-CoA oxidase gene (ACO-DR1) as a probe. As shown in Fig. 6, nucleoprotein complex bound by LOX1-GC was induced by 50 μM fenofibrate, which was inhibited by 100-fold excess amounts of unlabeled LOX1-GC or unlabeled ACO-DR1 that has been shown to bind activated PPARα [23,24]. Coincubation with an anti-PPARα antibody also abolished the complex formation, although control IgG did not. Furthermore, nucleoprotein complex bound by ACO-DR1 showed almost the same electrophoretic mobility (Fig. 6). These results indicate that activated PPARα can bind to the GC box motif in the promoter region of human LOX-1 gene and that its binding site for the GC box in the LOX-1 gene overlaps with that for the PPRE in the acyl-CoA oxidase gene.

Discussion

Previous studies have suggested that endothelial activation elicited by Ox-LDL and its lipid constituents may be involved in initiation and progression of atherosclerosis [25–27]. Ox-LDL uptake mediated by LOX-1 has been shown to induce cellular oxidative stress, activation of the proinflammatory transcription factor NF-κB [28], production of matrix metalloproteinases [29], expression of monocyte chemotactic protein-1 (MCP-1) [30], and cell apoptosis [31], which may potentially enhance atherosclerotic progression and stimulate rupture of atheromatous plaques.

On the other hand, PPARα and γ are also expressed by vascular endothelial cells and smooth muscle cells [11–14,17]. Previous reports have shown that PPARα ligands can suppress expression of proinflammatory genes, such as VCAM-1, IL-6, and COX-2, in vascular endothelial or smooth muscle cells [14,17,32]. PPARγ ligands increase PAI-1 expression in vascular endothelial cells [11] and induce CD36 expression in macrophages [15]. Target genes of PPARα are relatively confined to a group of genes which are involved in the metabolism of fatty acids [33–36] and lipoproteins [37,38]. In addition to these target genes, our study has revealed, for the first time, that LOX-1, a scavenger receptor for atherogenic Ox-LDL and other physiological ligands [39–41], is also a target of PPARα in vascular endothelial cells. Moreover, recent studies showed oxidized phospholipids, constitutes of Ox-LDL, directly activated PPARα to induce expression of MCP-1 and IL-8, which was completely abolished in endothelial cells from PPARα null mice [19]. LOX-1 expression is upregulated by Ox-LDL both in endothelial cells [42] and vascular smooth muscle cells [31]. In addition, suppression of LOX-1 inhibits Ox-LDL-induced MCP-1 expression in endothelial cells [30]. Thus, PPARα-induced LOX-1 expression might be involved in Ox-LDL-induced MCP-1 expression in atherogenesis.

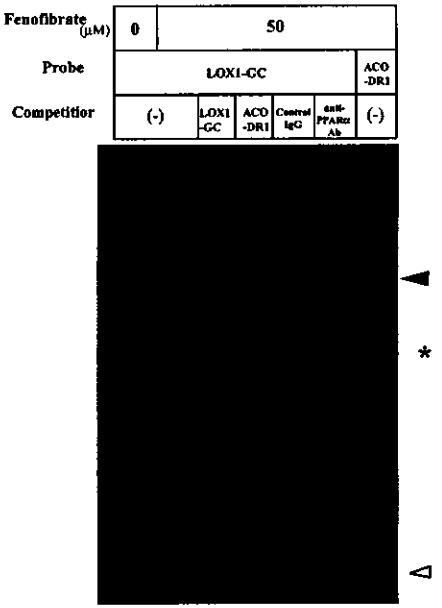

Fig. 6. Activated PPARα binds to the GC box in the LOX-1 promoter After treated with or without 50 or 100 μM of fenofibrate for 24 h, nuclear protein was extracted from BAECs and then subjected to EMSA. Double stranded ^{32}P-labeled nucleotides corresponding to GC box motif in LOX-1 promoter (LOX1-GC) or PPRE in rat acyl-CoA oxidase promoter (ACO-DR1) were used as probes as indicated. An antibody directed to PPARα, control IgG, and unlabeled competitor oligonucleotides were also added in the binding reaction as indicated. A closed arrowhead indicates the band induced by fenofibrate treatment and abolished by coincubation with unlabeled competitors or with anti-PPARα antibodies. An open arrowhead indicates free probe. An asterisk indicated a fenofibrate-induced shift band which was not suppressed by an anti-PPARα antibody.

In general, PPARs can stimulate gene transcription by heterodimer complex formation with RXR and its interaction with the *cis*-acting element, PPRE [43–45]. Although the consensus nucleotide sequence for PPRE was undetectable in the 5′ flanking region of the LOX-1 gene, we have identified, for the first time, the GC box motif as a responsible element for PPARα-induced gene transcription. However, in EMSA (Fig. 6) another inducible band by fenofibrate treatment was also visible below the PPAR band as indicated by the asterisk. This band was not reduced by addition of an anti-PPARα antibody; therefore, this band might correspond to another fenofibrate-inducible nuclear protein which can be bound to DR-1 sequence and the GC box motif. In addition, this report is the first to demonstrate transcriptional regulation of the LOX-1 gene. PPARα have been reported to regulate gene transcription by interacting with other transcription factors or cofactors, such as CBP [46], PGC-1 [47], and SRC-1 [48]. Therefore, transcriptional activation by PPARα via the GC box motif may be mediated by its interaction with cofactors other than RXR. This point needs to be further explored in the future.

In summary, the present report provides evidence, for the first time, that endothelial LOX-1 expression can be upregulated by PPARα via the GC box motif in the promoter region. Further studies would elucidate the pathophysiological relevance of PPARα ligand-induced endothelial LOX-1 expression in atherogenesis and other pathophysiological settings in vivo.

Acknowledgments

This work has been supported, in part, by the Center of Excellence Grant (No. 12CE2006) and Grants-in-Aid (Nos. 11838008, 11694266, 11307018, and 32644) from the Ministry of Education, Science and Culture of Japan, and Grant (No. RFTF97L00803) from the Japan Society for the Promotion of Science. We thank Kyoto Red Cross Blood Center for gifts of unused human plasma. We also to acknowledge Ms. Akemi Saito for her excellent technical assistance.

References

[1] T. Sawamura, N. Kume, T. Aoyama, H. Moriwaki, H. Hoshikawa, Y. Aiba, T. Tanaka, S. Miwa, Y. Katsura, T. Kita, T.

Masaki, An endothelial receptor for oxidized low-density lipoprotein, Nature 386 (1997) 73–77.
[2] N. Kume, H. Moriwaki, H. Kataoka, M. Minami, T. Murase, T. Sawamura, T. Masaki, T. Kita, Inducible expression of LOX-1, a novel receptor for oxidized LDL, in macrophages and vascular smooth muscle cells, Ann. N. Y. Acad. Sci. 902 (2000) 323–327.
[3] H. Moriwaki, N. Kume, H. Kataoka, T. Murase, E. Nishi, T. Sawamura, T. Masaki, T. Kita, Expression of lectin-like oxidized low density lipoprotein receptor-1 in human and murine macrophages: upregulated expression by TNF-alpha, FEBS Lett. 440 (1998) 29–32.
[4] N. Kume, T. Kita, Roles of lectin-like oxidized LDL receptor-1 and its soluble forms in atherogenesis, Curr. Opin. Lipidol. 12 (2001) 419–423.
[5] N. Kume, T. Murase, H. Moriwaki, T. Aoyama, T. Sawamura, T. Masaki, T. Kita, Inducible expression of lectin-like oxidized LDL receptor-1 in vascular endothelial cells, Circ. Res. 83 (1998) 322–327.
[6] M. Minami, N. Kume, H. Kataoka, M. Morimoto, K. Hayashida, T. Sawamura, T. Masaki, T. Kita, Transforming growth factor-beta(1) increases the expression of lectin- like oxidized low-density lipoprotein receptor-1, Biochem. Biophys. Res. Commun. 272 (2000) 357–361.
[7] T. Murase, N. Kume, R. Korenaga, J. Ando, T. Sawamura, T. Masaki, T. Kita, Fluid shear stress transcriptionally induces lectin-like oxidized LDL receptor-1 in vascular endothelial cells, Circ. Res. 83 (1998) 328–333.
[8] H. Kataoka, N. Kume, S. Miyamoto, M. Minami, H. Moriwaki, T. Murase, T. Sawamura, T. Masaki, N. Hashimoto, T. Kita, Expression of lectin like oxidized low-density lipoprotein receptor-1 in human atherosclerotic lesions, Circulation 99 (1999) 3110–3117.
[9] B. Desvergne, A. Ijpenberg, P.R. Devchand, W. Wahli, The peroxisome proliferator-activated receptors at the cross-road of diet and hormonal signalling, J. Steroid. Biochem. Mol. Biol. 65 (1998) 65–74.
[10] K. Schoonjans, B. Staels, J. Auwerx, The peroxisome proliferator-activated receptors (PPARS) and their effects on lipid metabolism and adipocyte differentiation, Biochim. Biophys. Acta 1302 (1996) 93–109.
[11] N. Marx, T. Bourcier, G.K. Sukhova, P. Libby, J. Plutzky, PPARgamma activation in human endothelial cells increases plasminogen activator inhibitor type-1 expression: PPARgamma as a potential mediator in vascular disease, Arterioscler. Thromb. Vasc. Biol. 19 (1999) 546–551.
[12] N. Marx, U. Schonbeck, M.A. Lazar, P. Libby, J. Plutzky, Peroxisome proliferator-activated receptor gamma activators inhibit gene expression and migration in human vascular smooth muscle cells, Circ. Res. 83 (1998) 1097–1103.
[13] S.M. Jackson, F. Parhami, X.P. Xi, J.A. Berliner, W.A. Hsueh, R.E. Law, L.L. Demer, Peroxisome proliferator-activated receptor activators target human endothelial cells to inhibit leukocyte-endothelial cell interaction, Arterioscler. Thromb. Vasc. Biol. 19 (1999) 2094–2104.
[14] B. Staels, W. Koenig, A. Habib, R. Merval, M. Lebret, I.P. Torra, P. Delerive, A. Fadel, G. Chinetti, J.C. Fruchart, J. Najib, J. Maclouf, A. Tedgui, Activation of human aortic smooth-muscle cells is inhibited by PPARalpha but not by PPARgamma activators, Nature 393 (1998) 790–793.
[15] P. Tontonoz, L. Nagy, J.G. Alvarez, V.A. Thomazy, R.M. Evans, PPARgamma promotes monocyte/macrophage differentiation and uptake of oxidized LDL, Cell 93 (1998) 241–252.
[16] S.A. Kliewer, S.S. Sundseth, S.A. Jones, P.J. Brown, G.B. Wisely, C.S. Koble, P. Devchand, W. Wahli, T.M. Willson, J.M. Lenhard, J.M. Lehmann, Fatty acids and eicosanoids regulate gene expression through direct interactions with peroxisome proliferator-activated receptors alpha and gamma, Proc. Natl. Acad. Sci. USA 94 (1997) 4318–4323.
[17] N. Marx, G.K. Sukhova, T. Collins, P. Libby, J. Plutzky, PPARalpha activators inhibit cytokine-induced vascular cell adhesion molecule-1 expression in human endothelial cells, Circulation 99 (1999) 3125–3131.
[18] P. Delerive, C. Furman, E. Teissier, J. Fruchart, P. Duriez, B. Staels, Oxidized phospholipids activate PPARalpha in a phospholipase A2-dependent manner, FEBS Lett. 471 (2000) 34–38.
[19] H. Lee, W. Shi, P. Tontonoz, S. Wang, G. Subbanagounder, C.C. Hedrick, S. Hama, C. Borromeo, R.M. Evans, J.A. Berliner, L. Nagy, Role for peroxisome proliferator-activated receptor alpha in oxidized phospholipid-induced synthesis of monocyte chemotactic protein-1 and interleukin-8 by endothelial cells, Circ. Res. 87 (2000) 516–521.
[20] N. Kume, H. Arai, C. Kawai, T. Kita, Receptors for modified low-density lipoproteins on human endothelial cells: different recognition for acetylated low-density lipoprotein and oxidized low-density lipoprotein, Biochim. Biophys. Acta 1091 (1991) 63–67.
[21] Z.F. Stephan, E.C. Yurachek, Rapid fluorometric assay of LDL receptor activity by Dil-labeled LDL, J. Lipid Res. 34 (1993) 325–330.
[22] M. Morimoto, N. Kume, S. Miyamoto, Y. Ueno, H. Kataoka, M. Minami, K. Hayashida, N. Hashimoto, T. Kita, Lysophosphatidylcholine induces early growth response factor-1 expression and activates the core promoter of PDGF-A chain in vascular endothelial cells, Arterioscler. Thromb. Vasc. Biol. 21 (2001) 771–776.
[23] M.C. Hunt, Y.Z. Yang, G. Eggertsen, C.M. Carneheim, M. Gafvels, C. Einarsson, S.E. Alexson, The peroxisome proliferator-activated receptor alpha (PPARalpha) regulates bile acid biosynthesis, J. Biol. Chem. 275 (2000) 28947–28953.
[24] J.D. Tugwood, I. Issemann, R.G. Anderson, K.R. Bundell, W.L. McPheat, S. Green, The mouse peroxisome proliferator-activated receptor recognizes a response element in the 5′ flanking sequence of the rat acyl CoA oxidase gene, EMBO J. 11 (1992) 433–439.
[25] R. Ross, The pathogenesis of atherosclerosis: a perspective for the 1990s, Nature 362 (1993) 801–809.
[26] M.A. Gimbrone Jr., M.I. Cybulsky, N. Kume, T. Collins, N. Resnick, Vascular endothelium. An integrator of pathophysiological stimuli in atherogenesis, Ann. N. Y. Acad. Sci. 748 (1995) 122–131, discussion 131–122.
[27] P. Libby, G.K. Hansson, Involvement of the immune system in human atherogenesis: current knowledge and unanswered questions, Lab. Invest. 64 (1991) 5–15.
[28] L. Cominacini, A.F. Pasini, U. Garbin, A. Davoli, M.L. Tosetti, M. Campagnola, A. Rigoni, A.M. Pastorino, V. Lo Cascio, T. Sawamura, Oxidized low density lipoprotein (ox-LDL) binding to ox-LDL receptor-1 in endothelial cells induces the activation of NF-kappaB through an increased production of intracellular reactive oxygen species, J. Biol. Chem. 275 (2000) 12633–12638.
[29] D. Li, L. Liu, H. Chen, T. Sawamura, S. Ranganathan, J.L. Mehta, LOX-1 mediates oxidized low-density lipoprotein-induced expression of matrix metalloproteinases in human coronary artery endothelial cells, Circulation 107 (2003) 612–617.
[30] D. Li, J.L. Mehta, Antisense to LOX-1 inhibits oxidized LDL-mediated upregulation of monocyte chemoattractant protein-1 and monocyte adhesion to human coronary artery endothelial cells, Circulation 101 (2000) 2889–2895.
[31] H. Kataoka, N. Kume, S. Miyamoto, M. Minami, M. Morimoto, K. Hayashida, N. Hashimoto, T. Kita, Oxidized LDL modulates Bax/Bcl-2 through the lectinlike Ox-LDL receptor-1 in vascular smooth muscle cells, Arterioscler. Thromb. Vasc. Biol. 21 (2001) 955–960.
[32] P. Delerive, K. De Bosscher, S. Besnard, W. Vanden Berghe, J.M. Peters, F.J. Gonzalez, J.C. Fruchart, A. Tedgui, G. Haegeman, B. Staels, Peroxisome proliferator-activated receptor alpha negatively

regulates the vascular inflammatory gene response by negative cross-talk with transcription factors NF-kappaB and AP-1, J. Biol. Chem. 274 (1999) 32048–32054.
[33] C. Mascaro, E. Acosta, J.A. Ortiz, P.F. Marrero, F.G. Hegardt, D. Haro, Control of human muscle-type carnitine palmitoyltransferase I gene transcription by peroxisome proliferator-activated receptor, J. Biol. Chem. 273 (1998) 8560–8563.
[34] K. Motojima, P. Passilly, J.M. Peters, F.J. Gonzalez, N. Latruffe, Expression of putative fatty acid transporter genes are regulated by peroxisome proliferator-activated receptor alpha and gamma activators in a tissue- and inducer-specific manner, J. Biol. Chem. 273 (1998) 16710–16714.
[35] K. Schoonjans, B. Staels, J. Auwerx, Role of the peroxisome proliferator-activated receptor (PPAR) in mediating the effects of fibrates and fatty acids on gene expression, J. Lipid Res. 37 (1996) 907–925.
[36] K. Schoonjans, M. Watanabe, H. Suzuki, A. Mahfoudi, G. Krey, W. Wahli, P. Grimaldi, B. Staels, T. Yamamoto, J. Auwerx, Induction of the acyl-coenzyme A synthetase gene by fibrates and fatty acids is mediated by a peroxisome proliferator response element in the C promoter, J. Biol. Chem. 270 (1995) 19269–19276.
[37] K. Schoonjans, J. Peinado-Onsurbe, A.M. Lefebvre, R.A. Heyman, M. Briggs, S. Deeb, B. Staels, J. Auwerx, PPARalpha and PPARgamma activators direct a distinct tissue-specific transcriptional response via a PPRE in the lipoprotein lipase gene, EMBO J. 15 (1996) 5336–5348.
[38] N. Vu-Dac, K. Schoonjans, V. Kosykh, J. Dallongeville, J.C. Fruchart, B. Staels, J. Auwerx, Fibrates increase human apolipoprotein A-II expression through activation of the peroxisome proliferator-activated receptor, J. Clin. Invest. 96 (1995) 741–750.
[39] T. Shimaoka, N. Kume, M. Minami, K. Hayashida, T. Sawamura, T. Kita, S. Yonehara, LOX-1 supports adhesion of Gram-positive and Gram-negative bacteria, J. Immunol. 166 (2001) 5108–5114.
[40] T. Shimaoka, N. Kume, M. Minami, K. Hayashida, T. Sawamura, T. Kita, S. Yonehara, Lectin-like oxidized low density lipoprotein receptor-1 (LOX-1) supports cell adhesion to fibronectin, FEBS Lett. 504 (2001) 65–68.
[41] K. Hayashida, N. Kume, M. Minami, T. Kita, Lectin-like oxidized LDL receptor-1 (LOX-1) supports adhesion of mononuclear leukocytes and a monocyte-like cell line THP-1 cells under static and flow conditions, FEBS Lett. 511 (2002) 133–138.
[42] T. Aoyama, H. Fujiwara, T. Masaki, T. Sawamura, Induction of lectin-like oxidized LDL receptor by oxidized LDL and lysophosphatidylcholine in cultured endothelial cells, J. Mol. Cell. Cardiol. 31 (1999) 2101–2114.
[43] I.J. A, E. Jeannin, W. Wahli, B. Desvergne, Polarity and specific sequence requirements of peroxisome proliferator-activated receptor (PPAR)/retinoid X receptor heterodimer binding to DNA. A functional analysis of the malic enzyme gene PPAR response element, J. Biol. Chem. 272 (1997) 20108–20117.
[44] H. Nakshatri, P. Bhat-Nakshatri, Multiple parameters determine the specificity of transcriptional response by nuclear receptors HNF-4, ARP-1, PPAR, RAR and RXR through common response elements, Nucleic Acids Res. 26 (1998) 2491–2499.
[45] P. Gervois, S. Chopin-Delannoy, A. Fadel, G. Dubois, V. Kosykh, J.C. Fruchart, J. Najib, V. Laudet, B. Staels, Fibrates increase human REV-ERBalpha expression in liver via a novel peroxisome proliferator-activated receptor response element, Mol. Endocrinol. 13 (1999) 400–409.
[46] R.M. Tolon, A.I. Castillo, A. Aranda, Activation of the prolactin gene by peroxisome proliferator-activated receptor-alpha appears to be DNA binding-independent, J. Biol. Chem. 273 (1998) 26652–26661.
[47] R.B. Vega, J.M. Huss, D.P. Kelly, The coactivator PGC-1 cooperates with peroxisome proliferator-activated receptor alpha in transcriptional control of nuclear genes encoding mitochondrial fatty acid oxidation enzymes, Mol. Cell. Biol. 20 (2000) 1868–1876.
[48] Y. Zhu, C. Qi, S. Jain, M.S. Rao, J.K. Reddy, Isolation and characterization of PBP, a protein that interacts with peroxisome proliferator-activated receptor, J. Biol. Chem. 272 (1997) 25500–25506.

Editorials

See related article, pages 370–376

Apoptosis of Vascular Cells by Oxidized LDL

Involvement of Caspases and LOX-1 and Its Implication in Atherosclerotic Plaque Rupture

Noriaki Kume, Toru Kita

Atherosclerotic plaque rupture followed by thrombus formation is a key event in the onset of acute coronary syndrome.[1] Apoptotic death of smooth muscle cells in the fibrous cap of the atherosclerotic plaque, in addition to degradation of extracellular matrix proteins by matrix metalloproteinases (MMPs), appears to be involved in atherosclerotic plaque rupture.[1] Oxidized LDL (Ox-LDL) has been implicated in the pathogenesis of atherosclerosis and atherosclerotic plaque rupture by promoting lipid accumulation, proinflammatory responses, and apoptotic cell death.[2–4] In fact, apoptotic cells are present in atherosclerotic lesions.[4,5] These biological effects, including proapoptotic effects, of Ox-LDL appear to be, at least in part, mediated by cell-surface receptors for Ox-LDL.[6]

Among several different classes of oxidized LDL receptors (also designated scavenger receptors) most of which are expressed mainly by macrophages, lectin-like oxidized LDL receptor-1 (LOX-1) is a type II membrane glycoprotein and expressed by activated vascular endothelial and smooth muscle cells, as well as macrophages.[7–10] LOX-1 expression can dynamically be induced by proinflammatory and other pathological stimuli relevant to atherogenesis.[11–14] Particularly, LOX-1 is induced by its ligand Ox-LDL,[15,16] as well as proinflammatory cytokines,[11,12] thus making a positive-feedback loop to enhance the effect of Ox-LDL on vascular cells. Uptake of Ox-LDL through LOX-1 induces reactive oxygen species (ROS), reduces nitric oxide, activates NF-κB,[17,18] and thereby upregulates expression of monocyte chemoattractant protein-1 (MCP-1) and MMPs.[19–21] LOX-1–dependent uptake of Ox-LDL also induces expression of a proapoptotic factor Bax, downregulates an antiapoptotic factor Bcl-2, and induces apoptosis of cultured vascular smooth muscle cells,[15] as well as endothelial cells.[16]

In human advanced atherosclerotic lesions, but not in normal arterial walls, macrophages and smooth muscle cells in the intima, in addition to vascular endothelial cells, dominantly express LOX-1,[22] which is colocalized with Bax.[15] In the early stages of atherogenesis, LOX-1 expression is prominent in vascular endothelial cells,[22,23] and apoptosis of endothelial cells also are detected, which may be implicated in endothelial dysfunction.[4] Thus, evidence has been accumulated to indicate that vascular cell apoptosis is mediated by Ox-LDL and its receptor LOX-1, and it may be crucial for atherosclerotic plaque rupture in the advanced stage, as well as endothelial dysfunction in the early stage.

However, molecular mechanisms involved in cell apoptosis by Ox-LDL and LOX-1 interactions have not been fully understood. In this issue of *Circulation Research*, Chen et al[24] have explored the involvement of caspases and the related molecules, such as Bcl-2 and c-IAP-2, and report that activation of caspase-9 and subsequent activation of caspase-3 are responsible for Ox-LDL–induced apoptosis of cultured vascular endothelial cells through its receptor LOX-1. In addition, release of mitochondrial apoptotic proteins, such as cytochrome *c* and Smac, was associated with Ox-LDL–induced caspase activation and apoptosis. Because Ox-LDL–induced release of cytochrome *c* or Smac was blocked by antisense oligonucleotides for LOX-1 but not affected by caspase inhibitors, cytochrome *c* and Smac appear to be upstream of caspase 9 and caspase 3 or might alternatively be independent of these caspases, although LOX-1 mediates the both pathways.

Chen et al[24] have confirmed that caspase 9 is upstream of caspase 3[25] in the Ox-LDL–induced apoptosis, as shown in cytochrome *c*–dependent apoptosis by other stimuli.[26] In addition, LOX-1–dependent downregulation of Bcl-2 by Ox-LDL is also shown in this study, as shown in cultured vascular smooth muscle cells.[15] Bcl-2 appears to be the upstream of cytochrome *c* and Smac and thus may inhibit their mitochondrial release. Furthermore, c-IAP-1, an inhibitor of caspase activation, has been shown to be downregulated by Ox-LDL, depending on LOX-1, in this study (Figure). LOX-1–dependent downregulation of Bcl-2 and c-IAP-1 may depend on ROS and its downstream signals; however, these points remain to be determined. Because activation of protein kinase C,[20] mitogen-activated protein (MAP) kinases,[19] and nuclear factor-κB (NF-κB)[17] and inhibition of phosphatidylinositol 3-kinase (PI3K)/Akt,[27] as well as production of ROS,[17] are involved in Ox-LDL and LOX-1–mediated cellular events, roles of these signal transduction cascades and transcription factors in Ox-LDL–induced downregulation of Bcl-2 and c-IAP-1, as well as cell apoptosis, should also be explored. In fact, PI3K/Akt has been implicated in Ox-LDL/LOX-1–induced apoptosis.[27,28] In addition, Bax is also the upstream of cytochrome *c* and Smac release and is upregulated by Ox-LDL–LOX-1 interactions,[15] signal transduction cascades, and transcription factors involved in Ox-LDL–induced upregulation of Bax should also be examined. More importantly, future studies should be conducted to determine the effect of vascular cell apoptosis in the pathogenesis of atherosclerotic plaque rupture, thrombus formation, and the onset of acute coronary syndrome in humans or suitable animal models in vivo.

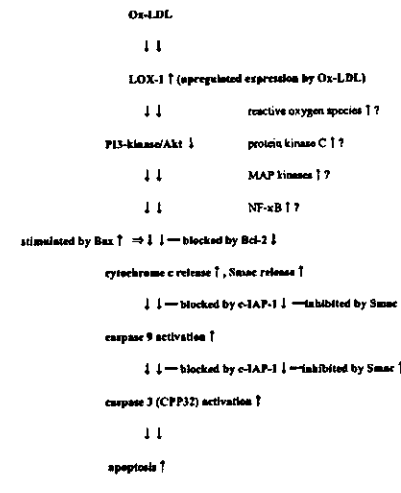

Molecular cascades involved in apoptosis by Ox-LDL–LOX-1 interactions.

The opinions expressed in this editorial are not necessarily those of the editors or of the American Heart Association.

From the Department of Cardiovascular Medicine, Graduate School of Medicine, Kyoto University, Kyoto, Japan.

Correspondence to Noriaki Kume, MD, PhD, Department of Cardiovascular Medicine, Graduate School of Medicine, Kyoto University, 54 Kawahara-cho, Shogoin, Sakyo-ku, Kyoto 606-8507, Japan. E-mail nkume@kuhp.kyoto-u.ac.jp

(*Circ Res.* 2004;94:269-270.)

Circulation Research is available at http://www.circresaha.org
DOI: 10.1161/01.RES.0000119804.92239.97

References

1. Libby P. Current concepts of the pathogenesis of the acute coronary syndromes. *Circulation.* 2001;104:365–372.
2. Ross R. Atherosclerosis: an inflammatory disease. *N Engl J Med.* 1999; 1340:115–126.
3. Steinberg D, Lewis A. Conner Memorial Lecture: oxidative modification of LDL and atherogenesis. *Circulation.* 1997;95:1062–1071.
4. Norata GD, Tonti L, Roma P, Catapano AL. Apoptosis and proliferation of endothelial cells in early atherosclerotic lesions: possible role of oxidised LDL. *Nutr Metab Cardiovasc Dis.* 2002;12:297–305.
5. Kockx MM, De Meyer GR, Muhring J, Jacob W, Bult H, Herman AG. Apoptosis and related proteins in different stages of human atherosclerosis and restenosis. *Circulation.* 1998;97:2307–2315.
6. Krieger M, Acton S, Ashkenas J, Pearson A, Penman M, Resnick D. Molecular flypaper, host defense, and atherosclerosis: structure, binding properties, and functions of macrophage scavenger receptors. *J Biol Chem.* 1993;268:4569–4572.
7. Sawamura T, Kume N, Aoyama T, Moriwaki H, Hoshikawa H, Aiba Y, Tanaka T, Miwa S, Katsura Y, Kita T, Masaki T. A novel endothelial receptor for oxidised low density lipoprotein. *Nature.* 1997;386:73–77.
8. Moriwaki H, Kume N, Sawamura T, Aoyama T, Hoshikawa H, Ochi H, Nishi E, Masaki T, Kita T. Ligand specificity of LOX-1, a novel receptor for oxidized low-density lipoprotein. *Arterioscler Thromb Vasc Biol.* 1998;18:1541–1547.
9. Kataoka H, Kume N, Miyamoto S, Murase T, Minami M, Sawamura T, Masaki T, Hashimoto N, Kita T. Biosynthesis and posttranslational processing of lectin-like oxidized LDL receptor-1 (LOX-1): N-linked glycosylation affects the cell-surface expression and the ligand binding. *J Biol Chem.* 2000;275:6573–6579.
10. Kume N, Kita T. Roles of lectin-like oxidized low density lipoprotein receptor-1 (LOX-1) and its soluble forms in atherogenesis. *Curr Opin Lipidol.* 2001;12:419–423.
11. Kume N, Murase T, Moriwaki H, Aoyama T, Sawamura T, Masaki T, Kita T. Inducible expression of lectin-like oxidized low density lipoprotein receptor-1 in vascular endothelial cells. *Circ Res.* 1998;83:322–327.
12. Minami M, Kume N, Kataoka H, Morimoto M, Hayashida K, Sawamura T, Masaki T, Kita T. Transforming growth factor-β1 increases the expression of lectin-like oxidized low density lipoprotein receptor-1. *Biochem Biophys Res Commun.* 2000;272:357–361.
13. Moriwaki H, Kume N, Kataoka H, Murase T, Nishi E, Sawamura T, Masaki T, Kita T. Expression of lectin-like oxidized low density lipoprotein receptor-1 in human and murine macrophages-upregulated expression by TNF-α. *FEBS Lett.* 1998;440:29–32.
14. Kita T. LOX-1, a possible clue to the missing link between hypertension and atherogenesis. *Circ Res.* 1999;84:1113–1115.
15. Kataoka H, Kume N, Miyamoto S, Minami M, Morimoto M, Hayashida K, Hashimoto N, Kita T. Oxidized low density lipoprotein (Ox-LDL) modulates Bax/Bcl-2 through lectin-like Ox-LDL receptor-1 in vascular smooth muscle cells. *Arterioscler Thromb Vasc Biol.* 2001;21:955–960.
16. Li D, Mehta JL. Upregulation of endothelial receptor for oxidized LDL (LOX-1) by oxidized LDL and implications in apoptosis of human coronary artery endothelial cells: evidence from use of antisense LOX-1 mRNA and chemical inhibitors. *Arterioscler Thromb Vasc Biol.* 2000; 20:1116–1122.
17. Cominacini L, Pasini AF, Garbin U, Davoli A, Tosetti ML, Campagnola M, Rigioni A, Pastorino AM, Lo Cascio V, Sawamura T. Oxidized low-density lipoprotein binding to LOX-1 in endothelial cells induces the activation of NF-κB through an increased production of intracellular reactive oxygen species. *J Biol Chem.* 2000;275:633–638.
18. Cominacini L, Rigoni A, Pasini AF, Garbin U, Davoli A, Campagnola M, Pastorino AM, Lo Cascio V, Sawamura T. The binding of oxidized low-density lipoprotein (ox-LDL) to ox-LDL receptor-1 reduces the intracellular concentration of nitric oxide in endothelial cells through an increased production of superoxide. *J Biol Chem.* 2001;276:13750–13755.
19. Li D, Mehta JL. Antisense to LOX-1 inhibits oxidized LDL-mediated upregulation of monocyte chemoattractant protein-1 and monocyte adhesion to human coronary artery endothelial cells. *Circulation.* 2000; 101:2889–2895.
20. Li D, Liu L, Chen H, Sawamura T, Ranganathan S, Mehta JL. LOX-1 mediates oxidized low-density lipoprotein-induced expression of matrix metalloproteinases in human coronary artery endothelial cells. *Circulation.* 2003;107:612–617.
21. Li D, Williams V, Liu L, Chen H, Sawamura T, Antakli T, Mehta JL. LOX-1 inhibition in myocardial ischemia-reperfusion injury: modulation of MMP-1 and inflammation. *Am J Physiol.* 2002;283:H1795–H1801.
22. Kataoka H, Kume N, Miyamoto S, Minami M, Moriwaki H, Sawamura T, Masaki T, Hashimoto N, Kita T. Expression of lectin-like oxidized low density lipoprotein receptor-1 in human atherosclerotic lesions. *Circulation.* 1999;99:3110–3117.
23. Chen M, Kakutani M, Minami M, Kataoka H, Kume N, Narumiya S, Kita T, Masaki T, Sawamura T. Increased expression of lectin-like oxidized low density lipoprotein receptor-1 in initial atherosclerotic lesions of Watanabe heritable hyperlipidemic rabbits. *Arterioscler Thromb Vasc Biol.* 2000;20:1107–1115.
24. Chen J, Mehta JL, Haider N, Zhang X, Narula J, Li D. Role of caspases in Ox-LDL–induced apoptotic cascade in human coronary artery endothelial cells. *Circ Res.* 2004;94:370–376.
25. Dimmeler S, Haendeler J, Galle J, Zeiher AM. Oxidized low-density lipoprotein induces apoptosis of human endothelial cells by activation of CPP32-like proteases. *Circulation.* 1997;95:1760–1763.
26. Slee EA, Harte MT, Kluck RM, Wolf BB, Casiano CA, Newmeyer DD, Wang HG, Reed JC, Nicholson DW, Alnemri ES, Green DR, Martin SJ. Ordering the cytochrome c-initiated caspase cascade: hierarchical activation of caspases-2, -3, -6, -7, -8, and -10 in a caspase-9-dependent manner. *J Cell Biol.* 1999;144:281–292.
27. Nakagawa T, Yasuda T, Hoshokawa H, Shimizu M, Kakinuma T, Chen M, Masaki T, Nakamura T, Sawamura T. LOX-1 expressed in cultured rat chondrocytes mediates oxidized LDL-induced cell death-possible role of dephosphorylation of Akt. *Biochem Biophys Res Commun.* 2002;299:91–97.
28. Li Y, Higashi Y, Itabe H, Song Y-H, Du J, Delafontaine P. Insulin-like growth factor-1 receptor activation inhibits oxidized LDL-induced cytochrome *c* release and apoptosis via the phosphatidylinositol 3 kinase/Akt signaling pathway. *Arterioscler Thromb Vasc Biol.* 2003;23:2178–2184.

KEY WORDS: oxidized LDL ■ caspases ■ apoptosis

ELSEVIER

Atherosclerosis 176 (2004) 289–296

ATHEROSCLEROSIS

www.elsevier.com/locate/atherosclerosis

Heparin-binding EGF-like growth factor induces expression of lectin-like oxidized LDL receptor-1 in vascular smooth muscle cells

Eri Mukai [a,b], Noriaki Kume [a,*], Kazutaka Hayashida [a], Manabu Minami [a], Yuichiro Yamada [b], Yutaka Seino [b], Toru Kita [a]

[a] *Department of Cardiovascular Medicine, Graduate School of Medicine, Kyoto University, 54 Kawahara-cho, Shogoin, Sakyo-ku, Kyoto 606-8507, Japan*
[b] *Department of Diabetes and Clinical Nutrition, Graduate School of Medicine, Kyoto University, 54 Kawahara-cho, Shogoin, Sakyo-ku, Kyoto 606-8507, Japan*

Received 1 May 2003; received in revised form 23 October 2003; accepted 30 March 2004

Available online 23 July 2004

Abstract

Receptor-mediated endocytosis of oxidized LDL (Ox-LDL) has been implicated in lipid accumulation and vascular cell dysfunction. Lectin-like Ox-LDL receptor-1 (LOX-1) is highly inducible by proinflammatory cytokines, as well as angiotensin II and Ox-LDL in vitro. LOX-1 is expressed in macrophages and smooth muscle cells accumulated in the intima of advanced atherosclerotic plaques in vivo. Here we show that heparin-binding epidermal growth factor-like growth factor (HB-EGF), a potent mitogen for vascular smooth muscle cells, induces LOX-1 expression in cultured bovine aortic smooth muscle cells. HB-EGF (1–100 ng/ml) induced LOX-1 expression, which was peaked between 8 and 16 h after HB-EGF stimulation. HB-EGF-induced expression of LOX-1 was suppressed by ZD1839, an inhibitor of EGF receptor phosphorylation. Both MEK and p38 mitogen-activated protein kinase (MAPK) inhibitors significantly blocked LOX-1 upregulation induced by HB-EGF. Phosphatidylinositol 3-kinase (PI3K) inhibitors also blocked HB-EGF-induced LOX-1 expression. HB-EGF induced phosphorylation of ERK, p38 MAPK and Akt, which were suppressed by ZD1839. Upregulated expression of LOX-1 was associated with enhanced uptake of DiI-labeled Ox-LDL in smooth muscle cells. Taken together, HB-EGF can also act as an inducer of LOX-1 expression and play an integral role in foam cell transformation, cellular dysfunction, and proliferation of smooth muscle cells in atherogenesis.

Keywords: Oxidized LDL; Scavenger receptors; LOX-1; HB-EGF; Vascular smooth muscle cells

1. Introduction

Several lines of evidence have suggested that oxidized LDL (Ox-LDL) appears to play key roles in atherogenesis [1,2]. Receptor-mediated binding and uptake of Ox-LDL may be crucial in activation of vascular cells, as well as lipid accumulation and subsequent foam cell transformation [3].

Several different classes of receptors for atherogenic Ox-LDL have been identified and characterized. Among them, lectin-like Ox-LDL receptor-1 (LOX-1) is a 40–50 kDa type II membrane protein with a C-type lectin-like extracellular domain and a short cytoplasmic tail, which was originally cloned in vascular endothelial cells [4]. LOX-1 can support binding, internalization, and degradation of Ox-LDL [5]. Subsequent studies have revealed that expression of LOX-1 can also be found in macrophages [6,7] and activated vascular smooth muscle cells [8–11] in culture. LOX-1 expression is not constitutive, but dynamically induced by proinflammatory cytokines, such as tumor necrosis factor (TNF) α [12] and transforming growth factor (TGF) β [13], angiotensin II [14,15], Ox-LDL [16,17], fluid shear stress [18] at the level of gene transcription. More importantly, LOX-1 is highly expressed by macrophages and smooth muscle cells accumulated in the intima of advanced atherosclerotic lesions, as well as endothelial cells covering early atherosclerotic lesions in vivo [19,20]. These data suggest that LOX-1 may play important roles in both endothelial activation and foam cell transformation of macrophages and vascular smooth muscle cells in atherogenesis.

Heparin-binding epidermal growth factor (EGF)-like growth factor (HB-EGF) is a potent mitogen for vascular smooth muscle cells, which can be expressed by macrophages, endothelial cells, as well as vascular smooth muscle cells [21–23]. HB-EGF can induce migration, proliferation, and phenotypic modulation of smooth muscle cells through its interaction with the EGF receptor [21,23]. Expression of HB-EGF can be induced by proinflammatory cytokines [24], angiotensin II [22], a phospholipid component of Ox-LDL [25–27], as well as fluid shear stress [28]. Furthermore, upregulated expression of HB-EGF in atherosclerotic lesions has also been demonstrated [29–31].

In the present study, therefore, we have tested the hypothesis if HB-EGF may induce expression of LOX-1 in vascular smooth muscle cells.

* Corresponding author. Tel.: +81-75-751-3623; fax: +81-75-751-4094.
E-mail address: nkume@kuhp.kyoto-u.ac.jp (N. Kume).

0021-9150/$ – see front matter © 2004 Elsevier Ireland Ltd. All rights reserved.
doi:10.1016/j.atherosclerosis.2004.03.028

2. Materials and methods

2.1. Materials

HB-EGF was purchased from R&D Systems. PD98059, SB203580, U0126, LY294002, and wortmannin were from Calbiochem. ZD1839 was a generous gift from AstraZeneca. A mouse anti-bovine LOX-1 monoclonal antibody was prepared by immunization with an recombinant bovine LOX-1 extracelluler domain as previously described [4]. A rat anti-human LOX-1 monoclonal antibody that cross-reacts with bovine LOX-1 was prepared by immunization with an recombinant human LOX-1 extracelluler domain generated by BAC TO BAC Baculovirus Expression System (Life Technologies). Antibodies for ERK and phosphorylated ERK were purchased from Cell Signaling, and antibodies for p38 mitogen-activated protein kinase (MAPK), phosphorylated p38 MAPK, Akt and phosphorylated Akt were from Santa Cruz Biotechnology. Irrelevant rat IgG was purchased from Chemicon.

2.2. Cell culture

Bovine aortic smooth muscle cells (BSMCs) were isolated by an explant method, after removing endothelial cells by scraping the inner surface of bovine aortas with a razor blade, and cultured in DMEM containing 10% (v/v) FBS. Cells were used for experiments at the passage levels between 2 and 6.

2.3. Immunoblot analysis

Cells were washed with phosphate-buffered saline (PBS) and lysed in PBS containing 1% Triton X-100. After heated at 95 °C for 5 min, equal protein concentrations of the cell lysates were subjected to SDS–polyacrylamide (12%) gel electrophoresis and transferred onto nitrocellulose membranes (PROTRAN, Schleicher & Schuell) by electroblotting. After preincubation with blocking buffer (PBS containing 0.1% Tween 20 and 5% nonfat dry milk) for 2 h at room temperature, blotted membranes were incubated with each primary antibody overnight at 4 °C, followed by washing twice with blocking buffer. Membranes were then incubated with a horseradish peroxidase-linked anti-mouse or anti-rabbit IgG (Amersham) for 1 h at room temperature, washed twice in PBS containing 0.04% Tween 20, and visualized by ECL Western blotting detection reagents (Amersham).

2.4. Northern blot analysis

Total cellular RNA was isolated by TRIZOL Reagent (Invitrogen). Total RNA (15 μg) was subjected to electrophoresis through 1% agarose gel containing formaldehyde, and transferred onto nitrocellulose membranes (OPTITRAN, Schleicher & Schuell). Membranes were hybridized with a *Xho*I fragment of bovine LOX-1 cDNA which had been labeled with [α-^{32}P] dCTP (Amersham) using random nonamer primers (Megaprime DNA labelling systems, Amersham).

2.5. Cellular uptake of DiI-labeled Ox-LDL

LDL (density: 1.019–1.063 g/ml) was isolated by sequential ultracentrifugation from human plasma. Oxidative modification of LDL was carried out with cupric ion in vitro. Oxidation was monitored by measuring the amount of thiobarbituric acid-reactive substances and electrophoretic mobility of the LDL particles. Our Ox-LDL contained approximately 10 nmol malondialdehyde equivalent/mg protein. Agarose gel electrophoresis showed increased electrophoretic mobility, which is almost equal to that of acetylated LDL, and minimal aggregation of the Ox-LDL particles. Labeling of Ox-LDL with 1,1′-dioctadecyl-3,3,3′,3′-tetramethylindocarbocyanine perchlorate (DiI, Molecular Probes) was performed as previously described [32]. To examine cellular uptake of Ox-LDL, confluent monolayers of BSMCs were incubated with DiI-labeled Ox-LDL (5 μg/ml) in DMEM/10% FBS for additional 2 h after treatment with the indicated reagents for 12 h and washed three times with the cell culture medium. Fluorescence microscopy was performed to detect DiI-Ox-LDL accumulated in cytoplasm.

2.6. Statistical analysis

Data are expressed as the mean ± standard deviations (S.D.). Statistical significance of the differences was evaluated by one-factorial ANOVA followed by Fisher's PLSD test, and $P < 0.05$ was considered significant.

3. Results

3.1. LOX-1 expression is upregulated by HB-EGF in cultured BSMCs

After BSMCs were treated with or without HB-EGF (0.01–100 ng/ml) for 16 h, total cell lysates were isolated

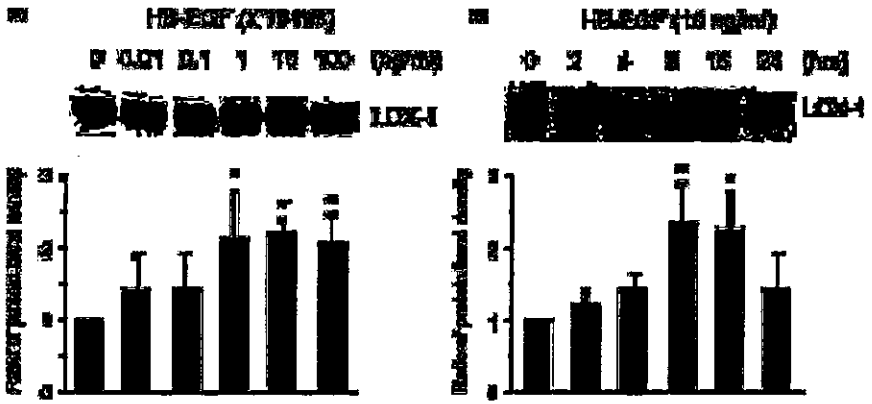

Fig. 1. Effects of HB-EGF on LOX-1 protein induction in BSMCs. After BSMCs were treated with the indicated concentrations of HB-EGF for 16 h (A), or with 10 ng/ml of the reagent for the indicated time periods (B), total cell lysates were subjected to immunoblot analyses with a mouse anti-LOX-1 monoclonal antibody. Data illustrated on the graph bar are the mean ± S.D. of four independent experiments, respectively. *$P < 0.005$ vs. 0 ng/ml of HB-EGF.

and subjected to immunoblot analyses. Fig. 1A demonstrates that LOX-1 protein levels were remarkably induced by HB-EGF in a concentration-dependent manner. Up-regulation of LOX-1 protein expression was observed at concentrations above 1 ng/ml of HB-EGF and peaked at 10 ng/ml of the regent, which resulted in 2.2-fold increase by densitometric analyses. LOX-1 protein expression was time-dependently induced by 10 ng/ml of HB-EGF; increased LOX-1 protein expression was detectable as early as 2 h after the addition of HB-EGF, peaked at 8–16 h (2.4- and 2.3-fold increases, respectively), and declined after 24 h (Fig. 1B).

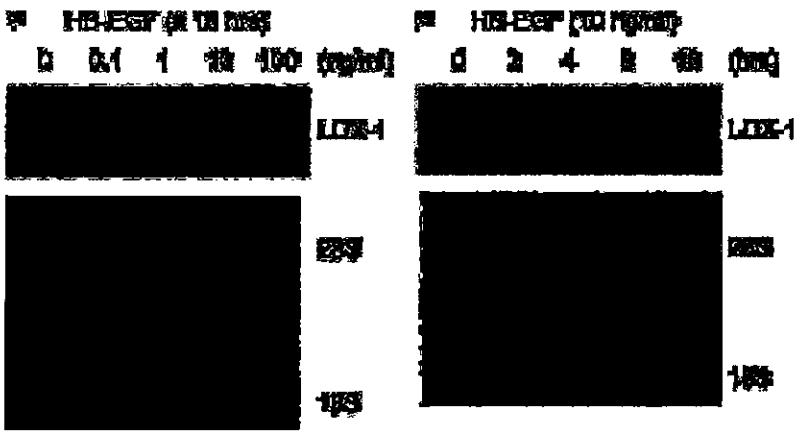

Fig. 2. Effects of HB-EGF on LOX-1 mRNA expression in BSMCs. After BSMCs were treated with the indicated concentrations of HB-EGF for 16 h (A), or with 10 ng/ml of the reagent for the indicated time periods (B), total cellular RNA was subjected to Northern blot analyses (15 μg RNA per lane) with ^{32}P-labeled cDNA probes. Bands for 28S and 18S ribosomal RNA visualized by ethidium bromide staining to control the amount of RNA loaded are also shown.

To determined whether increased expression of LOX-1 protein by HB-EGF depends upon induced expression of LOX-1 mRNA, Northern blot analyses were performed. As shown in Fig. 2A, HB-EGF increased the amount of LOX-1 mRNA concentration-dependently. Time-course experiments showed that increased levels of LOX-1 mRNA were detectable similarly to the protein expression (Fig. 2B).

3.2. HB-EGF increased the uptake of DiI-labeled Ox-LDL

To determine whether upregulated expression of LOX-1 by HB-EGF is correlated with enhanced uptake of Ox-LDL, uptake of DiI-labeled Ox-LDL into BSMCs were measured. After treatment with or without HB-EGF for 12 h, BSMCs were incubated with DiI-labeled Ox-LDL for additional 2 h. As shown in Fig. 3A, HB-EGF increased the internalization of DiI-Ox-LDL into BSMCs. The internalization of Di-Ox-LDL increased by HB-EGF was inhibited by the 100-fold excess amount of unlabeled Ox-LDL. Increased internalization of Di-Ox-LDL by HB-EGF was also inhibited by anti-LOX-1 monoclonal antibody (Fig. 3B). These results demonstrated that increases in LOX-1 expression by HB-EGF were associated with enhanced specific Ox-LDL uptake in BSMCs.

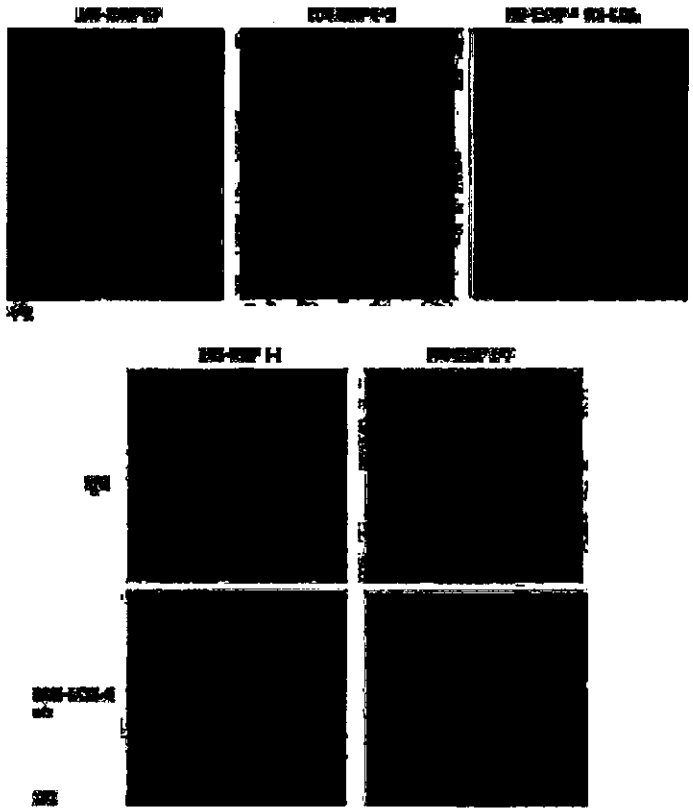

Fig. 3. HB-EGF increases the specific uptake of Ox-LDL in BSMCs. After treatment with or without 10 ng/ml of HB-EGF for 12 h, BSMCs were incubated with 5 μg/ml of DiI-labeled Ox-LDL for additional 2 h, in the presence or absence of 500 μg/ml of unlabeled Ox-LDL (A), and in the presence of a rat anti-LOX-1 monoclonal antibody or an irrelevant rat IgG (B). Representative pictures under fluorescence microscopy are shown.

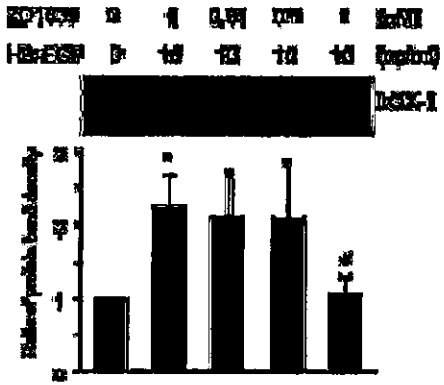

Fig. 4. HB-EGF-induced LOX-1 expression depends upon EGF receptor phosphorylation. After pretreatment with the indicated concentrations of ZD1839 for 1 h, BSMCs were treated with HB-EGF in the presence of ZD1839 for 10 h and then total cell lysates were subjected to Western blotting with a mouse anti-LOX-1 monoclonal antibody. Bar graphs indicate the mean ± S.D. of three independent experiments. $^{*}P < 0.001$, vs. 0 ng/ml of HB-EGF and $^{\#}P < 0.005$ vs. 10 ng/ml of HB-EGF.

3.3. HB-EGF-induced expression of LOX-1 depends upon EGF receptor phosphorylation

Previous studies have shown that EGF receptor phosphorylation mediates HB-EGF-dependent intracellular signal transduction. Therefore, we sought to determine if HB-EGF-induced LOX-1 expression depends upon EGF receptor phosphorylation. As shown in Fig. 4, ZD1839 (1 μM), an EGF receptor tyrosine kinase inhibitor that blocks EGF receptor phosphorylation [33], inhibited LOX-1 expression induced by HB-EGF to the basal level.

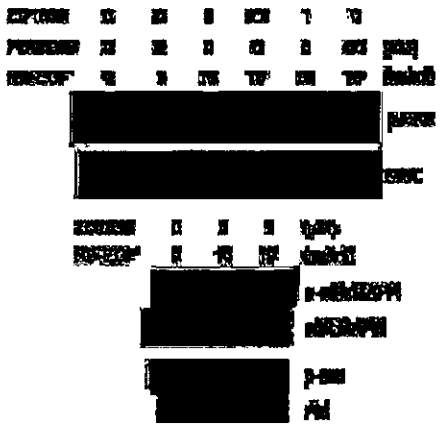

Fig. 5. HB-EGF induces phosphorylation of ERK, p38 MAPK and Akt. After pretreatment with the indicated concentrations of ZD1839 or PD98059 for 1 h, BSMCs were treated with HB-EGF in the presence of each reagent for 10 h and then total cell lysates were subjected to Western blotting with an anti-ERK, anti-phosphorylated ERK, anti-p38 MAPK, anti-phosphorylated p38 MAPK, anti-Akt or anti-phosphorylated Akt polyclonal antibody. A representative result from three independent experiments is shown.

3.4. HB-EGF induces phosphorylation of ERK, p38 MAPK and Akt depending upon EGF receptor phosphorylation

To determine whether HB-EGF, in fact, activates mitogen-activated protein kinases, such as ERK and p38 MAPK, or phosphatidylinositol 3-kinase (PI3K) in BSMCs, phosphorylation of ERK, p38 MAPK and Akt elicited by HB-EGF was measured. HB-EGF dose-dependently activated phosphorylation of ERK, as shown in Fig. 5. HB-EGF-induced

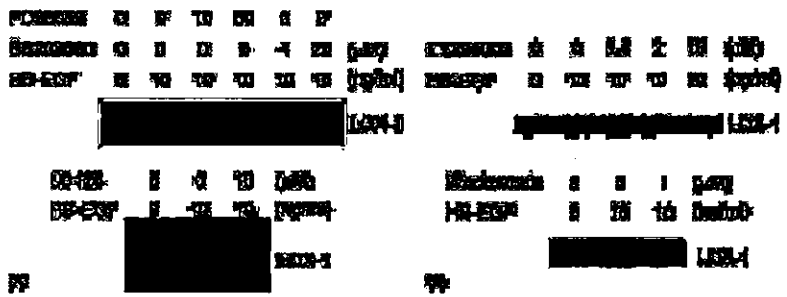

Fig. 6. HB-EGF-induced LOX-1 expression depends upon activation of MAPKs and PI3K. After pretreatment with the indicated concentrations of PD98059, SB203580, or U0126 (A), and LY294002 or wortmannin (B) for 1 h, BSMCs were treated with HB-EGF in the presence of each reagent for 10 h and then total cell lysates were subjected to Western blotting with a mouse anti-LOX-1 monoclonal antibody. A representative result from three independent experiments is shown.

ERK phosphorylation was suppressed by ZD1839, as well as PD98059, a MEK1 inhibitor, indicating the dependency upon EGF receptor phosphorylation. HB-EGF also slightly activated phosphorylation of p38 MAPK and Akt, which were suppressed by the EGF receptor phosphorylation inhibitor.

3.5. HB-EGF-induced expression of LOX-1 depends upon ERK, p38 MAPK and PI3K activation

We have further examined the dependency of HB-EGF-induced LOX-1 expression upon ERK and p38 MAPK as well as PI3K. As shown in Fig. 6A, both PD98059 and SB203580, inhibitors of MEK1 and p38 MAPK, respectively, significantly suppressed LOX-1 expression induced by HB-EGF. U0126, a strong and specific inhibitor of MEK1/2, also suppressed HB-EGF-induced LOX-1 expression. PI3K inhibitors, such as LY294002 and wortmannin, also suppressed HB-EGF-induced LOX-1 expression (Fig. 6B).

4. Discussion

Ox-LDL appears to play key roles in atherosclerotic progression and atherosclerotic plaque rupture. Effects of Ox-LDL on vascular cells appear to be mediated, at least in part, by Ox-LDL receptors, including LOX-1. In fact, LOX-1-mediated Ox-LDL uptake has been shown to induce cellular oxidative stress and activation of the proinflammatory transcription factor NF-κB[34] in vascular endothelial cells. In vascular smooth muscle cells, LOX-1-mediated uptake of Ox-LDL induces apoptosis [10], which may potentially stimulate rupture of atheromatous plaques in concert with other proinflammatory responses [35–37].

On the other hand, HB-EGF is a potent mitogen for smooth muscle cells, which is produced by vascular endothelial cells, smooth muscle cells, macrophages, and T lymphocytes [21–23]. HB-EGF has been shown to modulate smooth muscle phenotype, including induction of a macrophage colony-stimulating factor receptor (c-fms) [38]. Expression of HB-EGF can be induced by a variety of biological stimuli, including proinflammatory cytokines [24] and a phospholipid component in Ox-LDL [25–27]. Upregulated expression of HB-EGF and EGF receptors has been demonstrated in human atherosclerotic lesions [29–31], as well as animal models of vascular injury [39], thus suggesting a pivotal role in atherogenesis.

In the present study, we have shown that LOX-1, a receptor for atherogenic Ox-LDL, can be induced by HB-EGF in cultured vascular smooth muscle cells. Enhanced expression of LOX-1 in intimal smooth muscle cells, as well as endothelial cells, in atherosclerotic lesions has also been demonstrated previously [19,20]. Therefore, HB-EGF produced in the intima of atherosclerotic lesions may induce expression of LOX-1, and thereby enhance Ox-LDL-induced smooth muscle cell apoptosis, if abundant Ox-LDL is present, and thus may destabilize the atherosclerotic plaque and make it prone to rupture, although HB-EGF itself can also directly stimulate smooth muscle cell proliferation and inhibit apoptosis. This mechanism may represent one of the links between smooth muscle proliferation and lipid accumulation in atherogenesis, in addition to induced expression of HB-EGF by a lipid component of Ox-LDL [25–27].

Effects of HB-EGF on LOX-1 expression appear to be mediated by EGF receptor, because ZD1938, which blocks EGF receptor phosphorylation through inhibition of the receptor tyrosine kinase, suppressed HB-EGF-induced LOX-1 expression. In addition, both ERK and p38 MAPK, which are shown to be phosphorylated by HB-EGF, are involved in HB-EGF-induced LOX-1 expression, since PD98059, U0126, and SB203580 inhibited HB-EGF-induced LOX-1 expression. Furthermore, ERK and p38 MAPK phosphorylation by HB-EGF was suppressed by ZD1839, an inhibitor of EGF receptor tyrosine kinase. Moreover, PI3K is also involved in this process, because LY294002 and wortmannin inhibited HB-EGF-induced LOX-1 expression and HB-EGF, in fact, stimulated Akt phosphorylation. These results are consistent with previous reports showing that HB-EGF induces phosphorylation of EGF receptor and activates MAPK, and that HB-EGF-induced DNA synthesis is suppressed by PD98059 and LY294002 [40]. Although transcriptional regulatory mechanisms of LOX-1 gene have not been fully understood, oxidative stress has been implicated in LOX-1 gene induction [41,42]. Therefore, reactive oxygen species or redox-sensitive transcription factors may be upstream or downstream of MAPKs.

HB-EGF is a potent stimulus for smooth muscle cell migration and proliferation, and thus may modify atherosclerotic plaques into smooth muscle-rich stable ones. On the other hand, HB-EGF also induces LOX-1 which is a receptor for Ox-LDL and involved in Ox-LDL-induced apoptosis. Therefore, Ox-LDL might be a key factor to determine the stability of atherosclerotic plaques by modulating the function of smooth muscle cells, in addition to its actions on foam cell transformation and the production of matrix metalloproteinases.

In summary, the present report provides evidence, for the first time, that LOX-1 expression can be induced by HB-EGF in vascular smooth muscle cells. Further studies would elucidate the pathophysiological relevance of HB-EGF-induced smooth muscle LOX-1 expression in atherogenesis in vivo.

Acknowledgements

This work has been supported, in part, by the Center of Excellence Grant (No. 12CE2006) and a Research Grant (No. 14571092) from the Ministry of Education, Science

and Culture of Japan, Health and Labor Sciences Research Grant for Comprehensive Research on Aging and Health (H15-Choju-012) of Japan, and a research grant from Ono Medical Research Foundation, Japan. We thank Kyoto Red Cross Blood Center for gifts of unused human plasma. We also would like to acknowledge Ms. Akemi Saito for her excellent technical assistance.

References

[1] Witztum JL, Steinberg D. Role of oxidized low density lipoprotein in atherogenesis. J Clin Invest 1991;88:1785–92.
[2] Ross R. The pathogenesis of atherosclerosis: a perspective for the 1990s. Nature 1993;362:801–9.
[3] Steinberg D, Lewis A. Conner Memorial Lecture. Oxidative modification of LDL and atherogenesis. Circulation 1997;95:1062–71.
[4] Sawamura T, Kume N, Aoyama T, et al. An endothelial receptor for oxidized low-density lipoprotein. Nature 1997;386:73–7.
[5] Moriwaki H, Kume N, Sawamura T, et al. Ligand specificity of LOX-1, a novel endothelial receptor for oxidized low density lipoprotein. Arterioscler Thromb Vasc Biol 1998;18:1541–7.
[6] Moriwaki H, Kume N, Kataoka H, et al. Expression of lectin-like oxidized low density lipoprotein receptor-1 in human and murine macrophages: upregulated expression by TNF-alpha. FEBS Lett 1998;440:29–32.
[7] Yoshida H, Kondratenko N, Green S, Steinberg D, Quehenberger O. Identification of the lectin-like receptor for oxidized low-density lipoprotein in human macrophages and its potential role as a scavenger receptor. Biochem J 1998;334(Pt1):9–13.
[8] Draude G, Hrboticky N, Lorenz RL. The expression of the lectin-like oxidized low-density lipoprotein receptor (LOX-1) on human vascular smooth muscle cells and monocytes and its down-regulation by lovastatin. Biochem Pharmacol 1999;57:383–6.
[9] Aoyama T, Chen M, Fujiwara H, Masaki T, Sawamura T. LOX-1 mediates lysophosphatidylcholine-induced oxidized LDL uptake in smooth muscle cells. FEBS Lett 2000;467:217–20.
[10] Kataoka H, Kume N, Miyamoto S, et al. Oxidized LDL modulates Bax/Bcl-2 through the lectinlike Ox-LDL receptor-1 in vascular smooth muscle cells. Arterioscler Thromb Vasc Biol 2001;21:955–60.
[11] Kume N, Kita T. Apoptosis of vascular cells by oxidized LDL: involvement of caspases and LOX-1 and its implication in atherosclerotic plaque rupture. Circ Res 2004;94:269–70.
[12] Kume N, Murase T, Moriwaki H, et al. Inducible expression of lectin-like oxidized LDL receptor-1 in vascular endothelial cells. Circ Res 1998;83:322–37.
[13] Minami M, Kume N, Kataoka H, et al. Transforming growth factor-beta(1) increases the expression of lectin-like oxidized low-density lipoprotein receptor-1. Biochem Biophys Res Commun 2000;272:357–61.
[14] Morawietz H, Rueckschloss U, Niemann B, et al. Angiotensin II induces LOX-1, the human endothelial receptor for oxidized low-density lipoprotein. Circulation 1999;100:899–902.
[15] Li DY, Zhang YC, Philips MI, Sawamura T, Mehta JL. Upregulation of endothelial receptor for oxidized low-density lipoprotein (LOX-1) in cultured human coronary artery endothelial cells by angiotensin II type I receptor activation. Circ Res 1999;84:1043–9.
[16] Aoyama T, Fujiwara H, Masaki T, Sawamura T. Induction of lectin-like oxidized LDL receptor by oxidized LDL and lysophosphatidylcholine in cultured endothelial cells. J Mol Cell Cardiol 1999;31:2101–14.
[17] Li D, Mehta JL. Upregulation of endothelial receptor for oxidized LDL (LOX-1) by oxidized LDL and implications in apoptosis of human coronary artery endothelial cells: evidence from use of antisense LOX-1 mRNA and chemical inhibitors. Arterioscler Thromb Vasc Biol 2000;20:1116–22.
[18] Murase T, Kume N, Korenaga R, et al. Fluid shear stress transcriptionally induces lectin-like oxidized LDL receptor-1 in vascular endothelial cells. Circ Res 1998;83:328–33.
[19] Kataoka H, Kume N, Miyamoto S, et al. Expression of lectinlike oxidized low-density lipoprotein receptor-1 in human atherosclerotic lesions. Circulation 1999;99:3110–7.
[20] Chen M, Kakutani M, Minami M, et al. Increased expression of lectin-like oxidized low density lipoprotein receptor-1 in initial atherosclerotic lesion of Watanabe heritable hyperlipidemic rabbits. Arterioscler Thromb Vasc Biol 2000;20:1107–15.
[21] Higashiyama S, Abraham JA, Miller J, Fiddes JC, Klagsbrun M. A heparin-binding growth factor secreted by macrophage-like cells that is related to EGF. Science 1991;251:936–9.
[22] Temizer DH, Yoshizumi M, Perrella MA, Susanni EE, Quertermous T, Lee ME. Induction of heparin-binding epidermal growth factor-like growth factor mRNA by phorbol ester and angiotensin II in rat aortic smooth muscle cells. J Biol Chem 1992;267:24892–6.
[23] Raab G, Klagsbrun M. Heparin-binding EGF-like growth factor. Biochim Biophys Acta 1997;1333:F179–99.
[24] Yoshizumi M, Kourembanas S, Temizer DH, Cambria RP, Quertermous T, Lee ME. Tumor necrosis factor increases transcription of the heparin-binding epidermal growth factor-like growth factor gene in vascular endothelial cells. J Biol Chem 1992;267:9467–9.
[25] Kume N, Gimbrone Jr MA. Lysophosphatidylcholine transcriptionally induces growth factor gene expression in cultured human endothelial cells. J Clin Invest 1994;93:907–11.
[26] Nakano T, Raines EW, Abraham JA, Klagsbrun M, Ross R. Lysophosphatidylcholine upregulates the level of heparin-binding epidermal growth factor-like growth factor mRNA in human monocytes. Proc Natl Acad Sci USA 1994;91:1069–73.
[27] Nishi E, Kume N, Ochi H, et al. Lysophosphatidylcholine increases expression of heparin-binding epidermal growth factor-like growth factor in human T lymphocytes. Circ Res 1997;80:638–44.
[28] Monta T, Yoshizumi M, Kurihara H, Maemura K, Nagai R, Yazaki Y. Shear stress increases heparin-binding epidermal growth factor-like growth factor mRNA levels in human vascular endothelial cells. Biochem Biophys Res Commun 1993;197:256–62.
[29] Miyagawa J, Higashiyama S, Kawata S, et al. Localization of heparin-binding EGF-like growth factor in the smooth muscle cells and macrophages of human atherosclerotic plaques. J Clin Invest 1995;95:404–11.
[30] Nakata A, Miyagawa J, Yamashita S, et al. Localization of heparin-binding epidermal growth factor-like growth factor in human coronary arteries. Possible roles of HB-EGF in the formation of coronary atherosclerosis. Circulation 1996;94:2778–86.
[31] Reape TJ, Wilson VJ, Kanczler JM, Ward JP, Burnand KG, Thomas CR. Detection and cellular localization of heparin-binding epidermal growth factor-like growth factor mRNA and protein in human atherosclerotic tissue. J Mol Cell Cardiol 1997;29:1639–48.
[32] Stephan ZF, Yurachek EC. Rapid fluorometric assay of LDL receptor activity by DiI-labeled LDL. J Lipid Res 1993;34:325–30.
[33] Ranson M, Mansoor W, Jay son G. ZD1839 (IRES S A): a selective EGFR-TK inhibitor. Expert Rev Anticancer Ther 2002;2:161–8.
[34] Corrunacini L, Pasini AF, Garbin U, Davoli A, Tosetti ML, Campagnola M, et al. Oxidized low density lipoprotein (ox-LDL) binding to ox-LDL receptor-1 in endothelial cells induces the activation of NF-kappaB through an increased production of intracellular reactive oxygen species. J Biol Chem 2000;275:12633–8.
[35] Bjorkerud B, Bjorkerud S. Contrary effects of lightly and strongly oxidized LDL with potent promotion of growth versus apoptosis on arterial smooth muscle cells, macrophages, and fibroblasts. Arterioscler Thromb Vasc Biol 1996;16:416–24.
[36] Jovinge S, Crisby M, Thyberg J, Nilsson J. DNA fragmentation and ultrastructural changes of degenerating cells in atherosclerotic lesions and smooth muscle cells exposed to oxidized LDL in vitro. Arterioscler Thromb Vasc Biol 1997;17:2225–31.
[37] Bennett MR, Evan GI, Schwartz SM. Apoptosis of human vascular smooth muscle cells derived from normal vessels and coronary atherosclerotic plaques. J Clin Invest 1995;95:2266–74.
[38] Inaba T, Ishibashi S, Harada K, et al. Induction of macrophage colony-stimulating factor receptor (c-fms) expression in vascular medial smooth muscle cells treated with heparin binding epidermal growth factor-like growth factor. J Biol Chem 1996;271:24413–7.
[39] Igura T, Kawata S, Miyagawa J, et al. Expression of heparin-binding epidermal growth factor-like growth factor in neointimal cells induced by balloon injury in rat carotid arteries. Arterioscler Thromb Vasc Biol 1996;16:1524–31.
[40] Reynolds CM, Eguchi S, Frank GD, Motley ED. Signaling mechanisms of heparin-binding epidermal growth factor-like growth factor in vascular smooth muscle cells. Hypertension 2002;39:525–9.
[41] Nagase M, Ando K, Nagase T, Kaname S, Sawamura T, Fujita T. Redox-sensitive regulation of lox-1 gene expression in vascular endothelium. Biochem Biophys Res Commun 2001;281:720–5.
[42] Halvorsen B, Staff AC, Henriksen T, Sawamura T, Ranheim T. 8-*iso*-Prostaglandin F(2alpha) increases expression of LOX-1 in JAR cells. Hypertension 2001;37:1184–90.

Genetic subtypes of familial hemophagocytic lymphohistiocytosis: correlations with clinical features and cytotoxic T lymphocyte/natural killer cell functions

Eiichi Ishii, Ikuyo Ueda, Ryutaro Shirakawa, Ken Yamamoto, Hisanori Horiuchi, Shoulchi Ohga, Kenji Furuno, Akira Morimoto, Miyoko Imayoshi, Yoshiyasu Ogata, Masafumi Zaitsu, Masahiro Sako, Kenichi Koike, Akifumi Sakata, Hidetoshi Takada, Toshiro Hara, Shinsaku Imashuku, Takehiko Sasazuki, and Masaki Yasukawa

Mutations of the perforin (*PRF1*) and *MUNC13-4* genes distinguish 2 forms of familial hemophagocytic lymphohistiocytosis (FHL2 and FHL3, respectively), but the clinical and biologic correlates of these genotypes remain in question. We studied the presenting features and cytotoxic T lymphocyte/natural killer (CTL/NK) cell functions of 35 patients for their relationship to distinct FHL subtypes. FHL2 (n = 11) had an earlier onset than either FHL3 (n = 8) or the non-FHL2/FHL3 subtype lacking a *PRF1* or *MUNC13-4* mutation (n = 16). Deficient NK cell activity persisted after chemotherapy in all cases of FHL2, whereas some patients with FHL3 or the non-FHL2/FHL3 subtype showed partial recovery of this activity during remission. Alloantigen-specific CTL-mediated cytotoxicity was deficient in FHL2 patients with *PRF1* nonsense mutations, was very low in FHL3 patients, but was only moderately reduced in FHL2 patients with *PRF1* missense mutations. These findings correlated well with Western blot analyses showing an absence of perforin in FHL2 cases with *PRF1* nonsense mutations and of MUNC13-4 in FHL3 cases, whereas in FHL2 cases with *PRF1* missense mutations, mature perforin was present in low amounts. These results suggest an association between the type of genetic mutation in FHL cases and the magnitude of CTL cytolytic activity and age at onset. (Blood. 2005;105: 3442-3448)

Introduction

Hemophagocytic lymphohistiocytosis (HLH) is characterized by fever and hepatosplenomegaly associated with pancytopenia, hypertriglyceridemia, and hypofibrinogenemia.[1-3] Histologically, infiltrations of lymphocytes and histiocytes with hemophagocytic activity are seen in the reticuloendothelial system, bone marrow, and central nervous system (CNS).[4] HLH can be classified as either primary or secondary.[5] The primary form, also known as familial hemophagocytic lymphohistiocytosis (FHL), is inherited as an autosomal recessive disorder that usually arises during infancy.

Although generally attributed to uncontrolled T-cell activation leading to the excessive production of inflammatory cytokines and abnormal macrophage activation, the pathogenesis of HLH remains controversial.[6] Thus, identifying the molecular genetic defects that underlie HLH has been a major concern for many years. Recently, mutations of the perforin (*PRF1;* MIM170280) and *MUNC13-4* genes were found in patients with FHL.[7,8] Several reports indicated that the mutation in *PRF1* occurs in about 20% to 30% of patients with FHL, thus defining the FHL2 molecular subtype.[9-13] In Japan, *MUNC13-4* mutations were identified in 6 of 16 families with non-FHL2 subtypes, suggesting an FHL3 subtype that may account for as many as 20% to 25% of all FHL cases.[14] Attempts to identify molecular genetic defects in the 45% to 50% of FHL cases that lack both *PRF1* and *MUNC13-4* mutations are under way.

Natural killer (NK) cells and cytotoxic T lymphocytes (CTLs) both rely on the Fas-FasL system and the secretion of lytic granules containing granzyme and perforin to kill virus-infected and malignant cells. Perforin is synthesized as an inactive glycosylated precursor that is subsequently cleaved at the C-terminus to yield an active mature form.[15] Perforin protein in the form of a 534–amino acid polypeptide is constitutively expressed by NK cells and CTLs. In effector-target cell interactions, intracellular perforin is secreted by a mechanism of regulated exocytosis. The secreted perforin then becomes integrated into the target-cell membrane, followed by polymerization that generates poly-perforin pores in the presence of Ca^{2+} in the plasma membrane.[16,17] This pore formation leads to the destruction of cells by osmotic lysis and by allowing entry of apoptosis-inducing granzymes.[18] The perforin gene, *PRF1*, encodes transmembrane, endothelial growth factor–like, and C2 functional domains. The C2 domain binds to phospholipids in a Ca^{2+}-dependent manner, and proteolytic cleavage of the carboxy-terminal domain uncovers the C2 domain, allowing perforin to bind to the membrane.[15] Thus, perforin is produced as a precursor form, and posttranslational processing by proteolysis and glycosylation is required for its maturation.[15] Less is known about MUNC13-4, a homolog of MUNC13-1 that functions as a priming factor for neurotransmitter release. Because of its critical role in regulating the exocytosis of lytic granules in NK cells and CTLs, MUNC13-4 is expected to play a similar role in the exocytosis of perforin-containing vesicles.[19]

The onset of FHL typically occurs within the first year of life in 70% to 80% of cases[2,20]; examples of late-onset cases,[20] as well as a case in a teenager with genetic defects in *PRF1* in the absence of clinical symptoms,[21] have also been described. NK cell function was impaired in the majority of these cases, including those considered to be late onset.[20-22] These observations suggest that the defining characteristics of FHL may vary with both the type of genetic defect and the function of NK cells or CTLs.[23,24] We therefore analyzed the relationships among the clinical features, genetic defects, and CTL/NK cell functions of FHL patients with different molecular subtypes of this disease.

From the Department of Pediatrics, Saga University, Saga, Japan; Department of Pediatrics, Kyoto Prefectural University of Medicine, Kyoto, Japan; Department of Cardiovascular Medicine, Graduate School of Medicine, Kyoto University, Kyoto, Japan; Department of Pediatrics, Graduate School of Medicine, Kyushu University, Fukuoka, Japan; Division of Molecular Population Genetics, Department of Molecular Genetics, Medical Institute of Bioregulation, Kyushu University, Fukuoka, Japan; Division of Pediatrics, Osaka General Hospital, Osaka, Japan; Department of Pediatrics, Shinshu University, Matsumoto, Japan; Division of Pediatrics, Okinawa Central Hospital, Okinawa, Japan; Research Institute, International Medical Center of Japan, Tokyo, Japan; First Department of Internal Medicine, Ehime University, Ehime, Japan.

Submitted August 26, 2004; accepted December 30, 2004. Prepublished online as *Blood* First Edition Paper, January 4, 2005; DOI 10.1182/blood-2004-08-3296.

Supported by a Grant-in-Aid for Scientific Research in Japan.

Reprints: Eiichi Ishii, Department of Pediatrics, Faculty of Medicine, Saga University, 5-1-1 Nabeshima, Saga 849-8501, Japan; e-mail: ishiei@med.saga-u.ac.jp.

The publication costs of this article were defrayed in part by page charge payment. Therefore, and solely to indicate this fact, this article is hereby marked "advertisement" in accordance with 18 U.S.C. section 1734.

Patients, materials, and methods

Patients

A total of 67 Japanese patients with HLH (34 boys and 33 girls) were registered in the study from 1994 to 2003, 10 of whom were excluded because (i) the diagnosis was not compatible with FHL by criteria of the Histiocyte Society,[3] (ii) a blood sample was not obtained, or (iii) permission for the analysis was not given by the parents. Thus, 57 patients met the diagnostic criteria for FHL and had documented informed consent, fulfilling the principal requirements for eligibility. Informed consent was provided according to the Declaration of Helsinki. Thirty-five were tested for both *PRF1* and *MUNC13-4* mutations and were the focus of the presenting analysis. The study was approved by the institutional review boards at Kyushu University, Saga University, Ehime University, and Kyoto Prefectural University. Twenty-one patients received chemotherapy according to the HLH94 protocol, which specifies a combination of dexamethasone and etoposide as induction therapy, followed by dexamethasone, etoposide, and cyclosporine A as maintenance therapy.[25] Others were managed according to the best clinical judgment of their primary physicians. Subsequently, 22 patients underwent allogeneic hematopoietic stem cell transplantation (HSCT).

Flow cytometric and genetic analyses

To analyze perforin expression, we obtained peripheral blood mononuclear cells (PBMCs) before or during treatment and performed flow cytometric analysis as described in our previous reports.[11,13] Intracellular perforin was considered deficient when less than 1.0% of $CD3^+$, $CD8^+$, or $CD56^+$ cells expressed this antigen. When perforin expression was negative, we extracted genomic DNA and used it for sequencing analysis of *PRF1* by a previously described procedure with selected primers.[11,13] Polymerase chain reaction (PCR) products were subcloned and sequenced on the ABI PRISM 377 Sequence Detection System (PE-Applied Biosystems, Foster City, CA). When perforin expression was positive and/or *PRF1* mutations were absent we performed a genetic analysis for *MUNC13-4* mutations as described in our previous report.[14] Briefly, 28 primer sets were designed to amplify the 32 exons and flanking intronic sequences of the *MUNC13-4* gene from genomic DNA. PCR products were cloned into a TA cloning vector (Invitrogen, Carlsbad, CA), and the sequences were verified on an ABI3100 DNA sequencer (PE-Applied Biosystems).

Assay for NK cell activity

The NK cell activity of PBMCs was measured at diagnosis, during remission (between 2 and 6 months after diagnosis at completion of induction chemotherapy), and after HSCT by incubating cells with K562 targets for 4 hours with an effector-target (E/T) cell ratio of 20:1.[26] Target cells were also added to wells containing medium alone and to wells containing 1% Triton X-100 to determine the spontaneous and maximal levels of ^{51}Cr release, respectively. After 4 hours, 0.1 mL of supernatant was collected from each well. The percentage of specific ^{51}Cr release was calculated as (cpm experimental release − cpm spontaneous release)/(cpm maximal release − cpm spontaneous release) × 100, where cpm indicates counts per minute. At an E/T ratio of 20:1, normal values based on findings in 50 healthy children ranged from 18% to 40%, with 5% or less denoting a deficiency and 6% to 17% a moderate decrease.[26] NK cells were not routinely quantified; however, only specimens with PBM effector cell counts above 10^6 per tube were included in the analysis.

Generation of alloantigen-specific CTL lines and analysis of CTL cytotoxicity

Alloantigen-specific $CD8^+$ CTL lines were generated as previously described.[27,28] Briefly, PBMCs were obtained from FHL2 and FHL3 patients, their healthy parents, and unrelated healthy controls. These cells were cocultured with a mitomycin C (MMC)–treated B-lymphoblastoid cell line (B-LCL) established from an HLA-mismatched individual. Magnetized polystyrene beads coated with an anti-CD8 monoclonal antibody (DYNAL, Oslo, Norway) were used to isolate $CD8^+$ T lymphocytes from PBMCs that had been stimulated with allogeneic B-LCLs for 6 days. $CD8^+$ T lymphocytes, cultured in medium with interleukin-2 (Genzyme, Boston, MA), were stimulated with MMC-treated allogeneic B-LCLs 3 times at 1-week intervals; subsequently, these lymphocytes served as $CD8^+$ alloantigen-specific CTL lines. Alloantigen-specific CTL clones were generated from bulk CTL lines by a limiting dilution method as previously described.[27,28] The alloantigen specificity of CTL lines was determined by interferon-γ (IFN-γ) production in response to stimulation with allogeneic B-LCLs as described previously.[27,28] Briefly, 1×10^5 T lymphocytes were cocultured with or without 5×10^4 MMC-treated B-LCLs in 0.2 mL of RPMI 1640 medium supplemented with 10% fetal calf serum in a flat-bottomed microtiter well. In some experiments, an anti–HLA class I monoclonal antibody (w6/32) was added to wells at an optimal concentration. After 72 hours, the supernatant was collected from each well and assayed for the production of IFN-γ with an enzyme-linked immunosorbent assay (ELISA; ENDOGEN, Woburn, MA). Cytotoxic activity was determined by a 5-hour ^{51}Cr release assay as described earlier.[7] To evaluate the role of perforin in CTL-mediated cytotoxicity, we pretreated effector cells with an inhibitor of the perforin-based cytotoxic pathway, concanamycin A (CMA; Wako Pure Chemical Industries, Osaka, Japan), at a concentration of 100 nM for 2 hours before incubation with target cells.

Western blot analysis

T-cell lines established from FHL2 and FHL3 patients and a healthy control were used for Western blot analysis. Cell lysates were prepared by 1% Triton X-100 extraction. Then, the extracts (20 μg per lane each) were analyzed by the Western blot method with antiperforin (Lab Vision, Premont, CA) and anti-MUNC13-4 rabbit polyclonal antibodies.[19] Horseradish peroxidase–labeled anti-rabbit immunoglobulin G (IgG) polyclonal antibody was used as the secondary antibody with detection by enhanced chemiluminescence (Amersham Biosciences, Piscataway, NJ).

Statistical analysis

Differences in the distribution of categorical variables (eg, age at onset, family history, CNS involvement, NK cell activity at diagnosis, NK cell activity during remission, chemotherapy, and outcome) were analyzed with the Fisher exact test. When any significant variability ($P < .05$) was observed among the 3 subgroups (FHL2, FHL3, and non-FHL2/FHL3), additional analyses were done with the Bonferroni test to identify significant differences between discrete subgroup pairs. The Student *t* test was used to assess CTL lytic activity in 4 patient subgroups (FHL2 nonsense, FHL2 missense, FHL3, and healthy controls) at an E/T ratio of 10:1.

Results

Comparison of genotype and phenotype in 3 different molecularly defined subgroups

Since more than 80% of all FHL patients in Japan were registered by our study group over the 10-year accrual period, the findings of this analysis are believed to reflect the actual epidemiology of FHL in Japan. Of the 57 patients who met all eligibility criteria, 11 had *PRF1* mutations and lacked perforin expression by flow cytometry, whereas 46 were positive for perforin expression (Figure 1). Thus, the frequency of the FHL2 subtype in Japan can be estimated as 19% of all FHL cases. Twenty-four of the 46 patients with perforin expression were examined for *MUNC13-4* mutations and 8 (6 of whom were described in a previous report[14]) had a positive result, suggesting that the FHL3 subtype accounts for approximately one fourth of the FHL cases in Japan. The 16 patients with neither *PRF1* nor *MUNC13-4* mutation were classified as having non-FHL2/FHL3 disease.

Selected characteristics of patients with *PRF1* mutations (FHL2), *MUNC13-4* mutations (FHL3), or neither of these defects (non-FHL2/FHL3) are summarized in Table 1. The Fisher exact test demonstrated a significant difference in age at diagnosis among the 3 subgroups (Table 1). None of the other features examined (family history, CNS involvement, NK cell activity at diagnosis, type of chemotherapy, or outcome) showed any important variability. By the Bonferroni test, patients with the FHL2 subtype had an earlier age at disease onset ($P < .01$ for comparisons with both FHL3 and non-FHL2/FHL3).

Twenty-one patients were treated entirely on the HLH94 protocol whereas the remaining 14 received alterative therapy, including steroids, cyclosporine A, etoposide, and other cytotoxic drugs. There was partial recovery of deficient NK cell activity in the FHL3 and non-FHL2/FHL3 subgroups after induction chemotherapy or during remission compared with none in the FHL2 subgroup ($P < .05$ for FHL3; $P < .1$ for non-FHL2/FHL3). This improvement was not related to the type of chemotherapy administered. Full recovery of NK cell activity was noted in all 6 patients tested after HSCT, encompassing the FHL2, FHL3, and non-FHL2/FHL3 subgroups. Of the 22 patients who underwent allogeneic HSCT, 17 have survived for 10 months to 11 years (median, 4 years): 5 FHL2 patients, 4 FHL3 patients, and 8 non-FHL2/FHL3 patients. Thus, allogeneic HSCT was effective therapy in a majority of patients who underwent this procedure, regardless of the molecular subtype. By contrast, 8 of the 13 patients treated without HSCT have died; the remaining 5 have survived for 22 months to 7 years (median, 2 years 8 months).

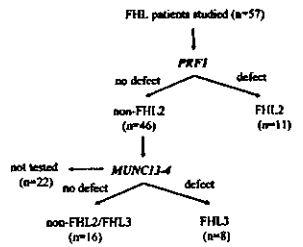

Figure 1. Classification of the FHL subtypes. *PRF1* mutations were initially classified in the 57 patients who fulfilled the diagnostic criteria of FHL. When perforin expression was positive or a *PRF1* mutation was absent, the samples were analyzed for a *MUNC13-4* mutations. The results allowed the FHL patients to be classified into 3 subtypes: FHL2 (n = 11), FHL3 (n = 8), and non-FHL2/FHL3 (n = 16).

Table 1. Characteristics of patients with the FHL2, FHL3, and non-FHL2/FHL3 subtypes of familial hemophagocytic lymphohistiocytosis

Category	No. patients with FHL2, n = 11	No. patients with FHL3, n = 8	No. patients with non-FHL2/FHL3, n = 16	P*
Age at diagnosis				.007
4-11 mo	0	6	5	
Family history				.513
Negative	6	3	10	
CNS involvement†				.713
Negative	4	3	3	
NK cell activity‡				.247
6%-17%	0	2	3	
Unknown	2	1	3	
Genetic mutation				
Nonsense/missense	1	0	0	
Donor site/donor site	0	1	0	
Acceptor site/acceptor site	0	2	0	
Acceptor site/nonsense	0	1	0	
Chemotherapy				.199
Various regimens	6	1	7	
Outcome				.292
Alive without HSCT	1	0	4	
Dead without HSCT	2	2	4	

CNS indicates central nervous system; NK, natural killer; nonsense, nonsense mutation including frameshift; missense, missense mutation; donor site, splice-donor site; acceptor site, splice-acceptor site; and HSCT, allogeneic hematopoietic stem cell transplantation.

*The Fisher exact test was used to determine the global *P* value for all 3 subgroups. By the Bonferroni test, patients with FHL2 had an earlier age at onset by comparison with either of the remaining subgroups ($P < .01$).

†Defined by neurologic symptoms and/or pleocytosis in cerebrospinal fluid.

‡NK cell activity measured at diagnosis and defined as deficient (≤ 6%), moderately decreased (6%-17%), or normal (18%-40%).

IFN-γ production and cytotoxic activity of T lymphocytes in patients with the FHL2 and FHL3 subtypes

Alloantigen-specific $CD8^+$ CTL lines were generated for all patients with available PBMCs (6 FHL2 and 2 FHL3). The antigen specificities of T-cell lines were initially examined by measuring IFN-γ production. As shown in Figure 2, all $CD8^+$ T-cell lines generated by stimulation with allogeneic B-LCLs (KIN-LCLs) produced large amounts of IFN-γ in response to stimulation with these lymphoblastoid cells but not with TAK-LCLs, which shared no HLA antigens with the KIN-LCLs. The production of IFN-γ by

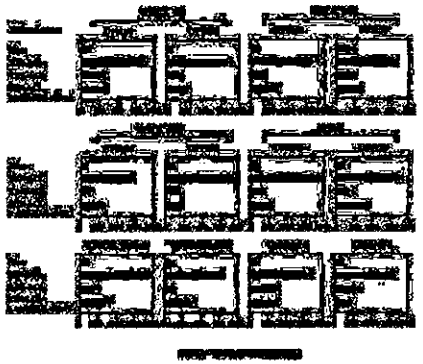

Figure 2. IFN-γ production by alloantigen-specific $CD8^+$ T-cell lines in response to stimulation with allogeneic B-LCLs. $CD8^+$ T-cell lines were generated from the PBMCs of the patients with FHL and healthy controls by stimulation with allogeneic B-LCLs (KIN-LCLs). Responder cells were cocultured with or without KIN-LCLs or TAK-LCLs, which shared no HLA antigens with KIN-LCLs, in the presence or absence of anti–HLA class I monoclonal antibody for 3 days. IFN-γ production was determined by ELISA; the results are mean values (± SD) from triplicate experiments. HLA types of B-LCLs were as follows: KIN-LCL, HLA-A01/30, B13/17, Cw6/–, DRB1*0701/*0701; TAK-LCL, HLA-A24/26, B62/–, Cw4/w9, DRB1*0405/*0901. NS indicates nonsense mutation; MS, missense mutation; and UPN, unique patient number.

the T-cell lines was clearly inhibited by anti–HLA class I monoclonal antibodies, indicating that the responses by these CTLs were alloantigen specific and HLA class I restricted.

Data on the cytotoxic activity of $CD8^+$ alloantigen-specific bulk T-cell lines generated from FHL2 and FHL3 patients, their healthy parents, and 2 healthy controls are shown in Figure 3. CTLs generated from the FHL2 patients with *PRF1* nonsense mutations (NSs; n = 2) were entirely deficient in antigen-specific cytotoxicity (percent cytotoxicity at E/T ratio of 10:1, mean 3.7 ± 1.1 SD), whereas those from the FHL3 patients (n = 2) showed very low but still detectable levels of this activity (mean 23.5 ± 2.1 SD). The cytotoxicity of CTLs generated from the patients with *PRF1* missense mutations (MSs; n = 4) was high (mean 44.0 ± 4.2 SD) compared with those of CTLs generated from FHL3 patients and patients with *PRF1* nonsense mutations but was clearly low compared with values for healthy controls and healthy parents with heterozygous mutations (mean 76.1 ± 4.7 SD). Although the patient sample in this comparison was small, statistical analysis indicated a significant difference in cytotoxicity between the FHL2 (NS)/FHL3 and FHL2 (MS) subgroups and between the FHL2 (MS) and the combined parent/healthy control groups ($P < .001$ for each comparison). Results similar to those in Figure 3 were obtained for alloantigen-specific CTL clones generated from the FHL patients and healthy controls (data not shown). The cytotoxicity of the $CD8^+$ CTL lines generated against allogeneic cells appeared to be mediated via the perforin-dependent pathway, since treatment of CTLs with CMA, a potent inhibitor of the perforin-mediated granule exocytosis cytolytic pathway, resulted in nearly complete inhibition of T-cell–mediated cytotoxicity.

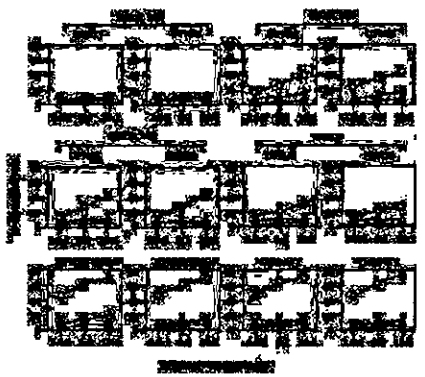

Figure 3. Cytotoxic activity of alloantigen-specific $CD8^+$ T-cell lines. $CD8^+$ T-cell lines were generated from PBMCs of the patients with FHL and healthy controls by stimulation with allogeneic B-LCLs (KIN-LCLs). Their cytotoxicity was determined against allogeneic KIN-LCLs in the presence (Δ) or absence (O) of CMA at a concentration of 100 nM and against allogeneic TAK-LCLs (●). Mean values and SD for triplicate experiments are reported. NS indicates nonsense mutation; MS, missense mutation; and UPN, unique patient number.

Western blot analysis for perforin and MUNC13-4 in the FHL2 and FHL3 subtypes

To account for the different patterns of CTL activity shown in Figure 3, we analyzed perforin expression in FHL patients whose CTL lines were established by Western blot analyses under reducing conditions (Figure 4A). Perforin in T cells from a healthy control and 2 FHL3 patients migrated at an apparent molecular mass of approximately 65 to 70 kDa. By contrast, the gene product associated with the *PRF1* nonsense mutation 1090.91delCT, present in 3 patients (UPN17, UPN24, and UPN42; Table 2), migrated at approximately 55 kDa. The gene product associated with the 207delC mutation (UPN24) was predicted to be an 84–amino acid peptide and therefore was too small to be seen. Gene products resulting from *PRF1* missense mutations 1228C>T (UPN42) and 1349C>T (UPN53 and UPN36) migrated at molecular masses similar to that of a healthy control, although the intensities of the bands appeared weaker compared with the control (Figure 4A). These results suggest that the mutant perforins were expressed in reduced amounts as full-length proteins with point mutations of R410W and T450M, respectively. Since a single band was also detected for UPN26 (a compound heterozygote with 949G>A and 1A>G; Table 2) at a position similar to the control, at least one of these mutants may be expressed as a full-length protein with a point mutation.

Figure 4. Perforin expression by Western blot analysis. Analysis is shown under reducing (A) or nonreducing (B) conditions in FHL patients. T cells from healthy control (C), FHL2 patients, and FHL3 patients were grown as described in "Generation of alloantigen-specific CTL lines and analysis of CTL cytotoxicity." Cell extracts of these cells (20 μg each) were analyzed by Western blot with antiperforin antibody. The data shown are representative results of 3 independent experiments. NS indicates nonsense mutation; and MS, missense mutation. The numbers above the lanes correspond to the UPNs of patients listed in Table 2.

Table 2. Relation of genotype to the cytotoxic functions of NK cells and CTLs in patients with the FHL2 or FHL3 subtypes

Subtype and UPN	Age/sex	Mutations	NK activity at diagnosis, % (% after treatment)	CTLs, %*	Western blot (active protein)	Outcome	HSCT
FHL2							
24	1 mo/F	1090.91delC/1207delC	1 (2)	3.9	Absent (p)	Alive	Y
53	7 y/F	1349C > T (mis)/1349C > T (mis)	0 (0)	46.5	Reduced (p)	Alive	Y
36†	1 mo/F	1349C > T (mis)/1349C > T (mis)	5 (5)	40.9	Reduced (p)	Alive	Y
FHL3							
23	5 mo/M	1596 + 1G > C/754 − 1G > C	19 (12)	23.8	Absent (m)	Dead	Y

Mutations in both alleles are listed in the table.
NK indicates natural killer; CTLs, cytotoxic T lymphocytes; p, perforin; mis, missense mutation; m, MUNC13-4 protein; Y, yes; N, no; and UPN, unique patient number.
*Mean CTL activity from 3 independent experiments at 10:1 of E/T ratio.
†FHL was diagnosed at 1 month of age, with relapse occurring 5 years later.

To identify the active mature form of perforin generated from the precursor of this protein, we performed Western blot analysis under nonreducing conditions (Figure 4B), as in a previous report.[15] Although the precursor forms of perforin (Figure 4B, upper bands) were detected in patients with *PRF1* missense mutations, FHL3 patients, and a healthy control, the active mature protein (Figure 4B, the lowest band) was markedly reduced in the patients with *PRF1* missense mutations, indicating that the proteolytic cleavage of perforin was inhibited. Under these conditions, the nonsense mutations (1090.91delCT and 207delC) did not yield a detectable band.

As shown in Figure 5, a single MUNC13-4 band of 120 kDa (expected size) was detected in a healthy control and all FHL2 patients but was missing in both of the FHL3 patients studied. Since the antibody used for the Western blot analysis was raised against the N-terminus of MUNC13-4 (1-262),[19] it is likely that the MUNC13-4 protein, even its N-terminal portion, was not expressed in the T cells of either of these 2 FHL3 patients.

Discussion

This study compared the frequencies, clinical features, genotypes, and CTL/NK cell functions of the FHL2 and FHL3 subtypes of familial hemophagocytic lymphohistiocytosis. Since more than 80% of all FHL cases in Japan were analyzed, the proportions of patients with *PRF1* or *MUNC13-4* mutations are likely to reflect the true epidemiology of this disorder. The FHL3 subtype appears more common than the FHL2 subtype (25% vs 19%), although this difference may vary depending on ethnic background and other factors.[9-13,29] Precise calculation of the frequency of each FHL subtype in countries outside of Japan is clearly needed.

Figure 5. MUNC13-4 expression by Western blot analysis in FHL patients. Cell extracts from the T cells of healthy control (C), FHL2, and FHL3 patients (20 μg each) were analyzed by Western blot with anti–MUNC13-4 antibody. The data represent 3 independent experiments. NS indicates nonsense mutation; and MS, missense mutation. The numbers above the lanes correspond to the UPNs of patients listed in Table 2.

FHL is sometimes difficult to diagnose when the patient is a first child or lacks an affected sibling. However, several clinical findings can support this diagnosis, including an age of less than 2 years, CNS involvement, and especially defective NK cell activity,[5] which has been observed in a majority of patients.[30-32] Comparison of NK cell activity among the FHL2, FHL3, and non-FHL2/FHL3 subtypes at diagnosis did not reveal any significant differences, as most of the evaluable cases were deficient or low in this activity. However, none of the FHL2 patients showed any recovery of NK cell activity after chemotherapy, in contrast to the FHL3 and non-FHL2/FHL3 subgroups. There was no apparent relationship between the recovery of functional NK cells and the type of chemotherapy received by these patients. Our findings agree with a recent report by Schneider et al,[24] who classified patients into 4 types according to the level of NK cell activity. All cases with *PRF1* homozygous nonsense mutations lacked any evidence of NK cell activity, regardless of the type of stimulation or the length of culture.[24] Thus, *PRF1* mutations appear to play an important role in the persistence of deficient NK cell activity in FHL.[32] Whether the transience of this deficiency in the FHL3 subtype is associated with *MUNC13-4* or still unidentified mutations, or perhaps a combination of the 2, remains to be determined. The partial recovery of NK cell activity may be associated with an increased number of NK cells or their release from the external suppressive effects of chemotherapy.

Perforin deficiency in FHL2 causes severe immune defects through defective NK and CTL activities.[6,30,31] A lack of perforin expression in $CD8^+$ T cells and/or NK cells by flow cytometric analysis generally correlates with mutated *PRF1* sequences.[10,13] However, Molleran Lee et al[32] recently reported cases of late-onset FHL with *PRF1* mutations but positive expression of perforin by flow cytometry. We identified 3 novel missense mutations of *PRF1* in this study: 949G>A, 1228C>T, and 1349C>T (Table 2), and each of the affected patients, except UPN36, showed late-onset clinical manifestations. In contrast to a previous report,[33] perforin expression by $CD8^+$ or $CD56^+$ cells in our study was also negative in all patients with *PRF1* missense mutations. Feldmann et al[12] characterized the genotype and phenotype of FHL2 patients; clinical and biologic analyses did not distinguish between patients with *PRF1* nonsense or missense mutations, although age at diagnosis was delayed in patients in the missense mutation group. It was also reported that several patients with late-onset disease had missense mutations of *PRF1*.[21,34]

In the FHL2 patients with *PRF1* missense mutations, we detected a mutant form of perforin whose molecular mass was similar to that of the wild-type protein by Western blot analysis under reducing conditions; however, as shown in Figure 4B, there was no mature form of the perforin proteins in these cases. McCormick et al[35] generated the 3-dimensional structure of the T435M *PRF1* mutant using comparative molecular modeling techniques applied to data from a single FHL patient. Their results predicted that the ability of the protein to bind Ca^{2+}, and hence its cytolytic function, would be strongly compromised. Katano et al[36] demonstrated the accumulation of an uncleaved precursor form of perforin in a patient with a *PRF1* missense mutation. Using Western blot analysis under nonreducing conditions we showed that the active mature form of perforin, the only form localized in lytic granules,[15] was absent in *PRF1* nonsense mutations and definitely reduced in all patients with *PRF1* missense mutations. These findings suggest that the missense mutations of *PRF1* lead to conformational changes in the perforin molecule that inhibit proteolytic cleavage of perforin precursors.

In our study, the cytotoxic function of CTLs in patients with *PRF1* missense mutations remained relatively intact compared with that associated with nonsense mutations of this gene. By contrast, all patients with any type of *PRF1* mutation showed a persistent deficiency in NK cell activity. Since the number and cytotoxic function of NK cells can vary depending on numerous factors, including the nature of the disease, infections, and type of treatment, measurements of NK cell activity in FHL2 cases may not accurately reflect the immune status of patients. We therefore established antigen-specific CTL lines from patients with the different subtypes of FHL and compared their cytotoxic activities. Since most of the patients with FHL are young children with an immunodeficient status, generating CTLs that are specific for viral or other recall antigens can be quite difficult; hence, we elected to generate alloantigen-specific CTL lines. The levels of cytotoxicity mediated by alloantigen-specific CTLs generated from patients with *PRF1* nonsense or missense mutations or with *MUNC13-4* mutations were clearly distinguishable from each other. Although many previous studies have relied on NK cells to examine cytolytic mediators in FHL, our findings suggest that functional analysis of antigen-specific CTLs may yield more useful insights into the immune competence of patients. Further studies with larger patient samples are needed to clarify the benefits of CTL assays in each subtype of FHL.

MUNC13-4 is a member of the *Munc13* gene family, which is required for neurotransmitter release in the small nematode *Caenorhabditis elegans*.[37] Feldmann et al[8] demonstrated that the MUNC13-4 protein colocalizes with cytotoxic granules near the site of contact between T lymphocytes and their targets and that granule exocytosis is blocked at a post-RAB27A stage in CTLs from FHL3 patients. We recently demonstrated that MUNC13-4 is a direct target of guanosine triphosphate–RAB27.[19] MUNC13-4 deficiency also results in defective cytolytic granule exocytosis despite polarization of the secretory granules and docking with the plasma membrane.[8] When we compared the cytotoxic activity of CTLs with *PRF1* or *MUNC13-4* mutations, the latter showed a lower affinity for target cells than did CTLs with *PRF1* missense mutations. The MUNC13-4 protein was not detected by Western blot analysis, indicating that its function was completely eliminated in FHL3 patients. The difference in the cytotoxic activity of CTLs may reflect the functions of the molecules responsible for FHL pathogenesis: while MUNC13-4 is a regulator of exocytosis in perforin-containing vesicles, perforin is the killing tool itself.

The only accepted curative therapy for FHL is allogeneic HSCT. Although the outcome of therapy did not differ between patients with the FHL2 or FHL3 subtype, 1 child with a *PRF1* missense mutation and 4 in the non-FHL2/FHL3 subgroup have survived without HSCT. Thus, early recognition of informative genetic defects and the cytotoxic activity of CTLs in cases of FHL may identify patients who could be spared the toxic effects of intensive chemotherapy with stem cell rescue.

Recent molecular genetic findings have demonstrated the diversity of FHL pathogenesis, but very little is known about the clinical and biologic correlations of the genetic subtypes of this disease. Although we observed a significant difference in age at onset and NK cell recovery between the FHL2 and FHL3 variants, further distinctions could not be made with any certainty. Nonetheless, the results of CTL assays performed on T-cell lines from a limited number of patients suggested an association with clinical features, type of mutation, and the subsequent production of functional proteins in FHL patients. If confirmed by studies of additional cases, the use of CTL assays to monitor the immune status of FHL patients might aid in the selection of therapy for cases without a documented genetic defect.

Acknowledgments

We thank John Gilbert for critical comments and editorial assistance; Naoko Kinukawa, Department of Medical Informatics, Kyushu University, Japan for statistical analysis of clinical parameters; and all of the members of the Japan HLH Study Group for their contributions to careful follow-up and data collection in each case. A complete list of the members of the Japan HLH Study Group appears in the "Appendix."

Appendix

The members of the Japan HLH Study Group were as follows. Yukiko Tsunematsu, MD, Department of Hematology, National Children's Hospital, Tokyo, Japan; Shuki Mizutani, MD, Department of Pediatrics, Tokyo Medical and Dental University, Tokyo, Japan; Naoko Kinukawa, Department of Pediatrics, Showa University, Tokyo, Japan; Hirokazu Kanegane, MD, Department of Pediatrics, Toyama Medical and Pharmaceutical University, Toyama, Japan; Keizo Horibe, MD, Clinical Research Center, National Nagoya Hospital, Nagoya, Japan; Ikuyo Ueda, MD and Akira Morimoto, MD, Kyoto Prefectural University, Kyoto, Japan; Naoki Sakata, MD, Department of Pediatrics, Kinki University, Osaka, Japan; Shinsaku Imashuku, MD, Department of Pediatrics, Takasago Seibu Hospital, Hyogo, Japan; Masaki Yasukawa, MD, Department of First Internal Medicine, Ehime University, Ehime, Japan; Shouichi Ohga, MD, and Toshiro Hara, MD, Department of Pediatrics, Kyushu University, Fukuoka, Japan; Nobuhiro Kimura, MD, First Department of Internal Medicine, Fukuoka University, Fukuoka, Japan; and Eiichi Ishii, MD, Department of Pediatrics, Saga University, Saga, Japan.

References

1. Loy TS, Diaz-Arias AA, Perry MC. Familial erythrophagocytic lymphohistiocytosis. Semin Oncol. 1991;18:34-39.
2. Janka GE. Familial erythrophagocytic lymphohistiocytosis. Eur J Pediatr. 1983;140:221-230.
3. Henter J, Elinder G, Ost A. Diagnostic guidelines for hemophagocytic lymphohistiocytosis. Semin Oncol. 1991;18:29-33.
4. Caballes RL, Caballes-Ponce MG, Kim DU. Familial hemophagocytic lymphohistiocytosis (FHLH). Pathology. 1997;29:92-95.
5. Filipovich AH. Hemophagocytic lymphohistiocytosis: a lethal disorder of immune regulation. J Pediatr. 1997;130:337-338.
6. Arico M, Danesino C, Pende D, Moretta L. Pathogenesis of hemophagocytic lymphohistiocytosis. Br J Haematol. 1991;114:761-769.
7. Stepp SE, Dufourcq-Lagelouse R, Le Deist F, et al. Perforin gene defects in familial hemophagocytic lymphohistiocytosis. Science. 1999;286: 1957-1959.
8. Feldmann J, Callebaut I, Raposo G, et al. Munc13-4 is essential for cytolytic granules fusion and is mutated in a form of familial hemophagocytic lymphohistiocytosis (FHL3). Cell. 2003;115:461-473.
9. Gorananedottar Ericson K, Fadeeal B, Nilsson-Ardnor S, et al. Spectrum of perforin gene mutations in familial hemophagocytic lymphohistiocytosis. Am J Hum Genet. 2001;68:590-597.
10. Kogawa K, Lee SM, Villanueva J, Marmer D, Sumegi J, Filipovich AH. Perforin expression in cytotoxic lymphocytes from patients with hemophagocytic lymphohistiocytosis and their family members. Blood. 2002;99:61-66.
11. Suga N, Takada H, Ohga S, et al. Perforin defects of primary haemophagocytic lymphohistiocytosis in Japan. Br J Haematol. 2002;118:346-349.
12. Feldmann J, Le Deist F, Ouachee-Chardin M, et al. Functional consequences of perforin gene mutations in 22 patients with familial haemophagocytic lymphohistiocytosis. Br J Haematol. 2002; 117:965-972.
13. Ueda I, Morimoto A, Inaba T, et al. Characteristic perforin gene mutations of haemophagocytic lymphohistiocytosis patients in Japan. Br J Haematol. 2003;121:503-510.
14. Yamamoto K, Ishii E, Sako M, et al. Identification of novel MUNC13-4 mutations in familial hemophagocytic lymphohistiocytosis and functional analysis of MUNC13-4-deficient cytotoxic T lymphocytes. J Med Genet. 2004;41:783-787.
15. Uellner R, Zvelebil MJ, Hopkins J, et al. Perforin is activated by a proteolytic cleavage during biosynthesis which reveals a phospholipid-binding C2 domain. EMBO J. 1997;16:7287-7296.
16. Podack ER, Young JD, Cohn ZA. Isolation and biochemical and functional characterization of perforin 1 from cytolytic T-cell granules. Proc Natl Acad Sci U S A. 1985;82:8629-8633.
17. Masson D, Peters PJ, Geuze HJ, Borst J, Tschopp J. Interaction of chondroitin sulfate with perforin and granzymes of cytotoxic T-cells is dependent on pH. Biochemistry. 1990;29:11229-11235.
18. Darmon AJ, Nicholson DW, Bleackley RC. Activation of the apoptotic protease CPP32 by cytotoxic T-cell-derived granzyme B. Nature. 1995;377: 446-448.
19. Shirakawa R, Higashi T, Tabuchi A, et al. Munc13-4 is a GTP-Rab27 binding protein regulating dense core granule secretion in platelets. J Biol Chem. 2004;279:10790-10737.
20. Allen M, de Fusco C, Legrand F, et al. Familial hemophagocytic lymphohistiocytosis: how late can the onset be? Haematologica. 2001;86:499-503.
21. Clementi R, Emmi L, Maccario R, et al. Adult onset and atypical presentation of hemophagocytic lymphohistiocytosis in siblings carrying PRF1 mutations. Blood. 2002;100:2266-2267.
22. Elle R, Janka GE, Belohradsky BH. Natural killer cell function and interferon production in familial hemophagocytic lymphohistiocytosis. Pediatr Hematol Oncol. 1989;6:265-272.
23. Arico M, Janka G, Fischer A, et al. Hemophagocytic lymphohistiocytosis: report of 122 children from the International Registry. Leukemia. 1996; 10:197-203.
24. Schneider EM, Lorenz I, Muller-Rosenberger M, Steinbach G, Kron M, Janka-Schaub GE. Hemophagocytic lymphohistiocytosis (HLH) is associated with deficiencies of cellular cytolysis but normal expression of apoptosis related transcripts. Blood. 2002;100:2891-2898.
25. Henter JI, Arico M, Egeler RM, et al. HLH-94: a treatment protocol for hemophagocytic lymphohistiocytosis. HLH Study Group of the Histiocyte Society. Med Pediatr Oncol. 1997;28:342-347.
26. Imashuku S, Hyakuna N, Funabiki T, et al. Low natural killer activity and central nervous system disease as a high-risk prognostic indicator in young patients with hemophagocytic lymphohistiocytosis. Cancer. 2002;94:3023-3031.
27. Yasukawa M, Ohminami H, Arai J, Kasahara Y, Ishida Y, Fujita S. Granule exocytosis, and not the fas/fas ligand system, is the main pathway of cytotoxicity mediated by alloantigen-specific CD4(+) as well as CD8(+) cytotoxic T lymphocytes in humans. Blood. 2000;95:2352-2355.
28. Yanai F, Ishii E, Kojima K, et al. Essential roles of perforin in antigen-specific cytotoxicity mediated by human CD4+ T lymphocytes: analysis using the combination of hereditary perforin-deficient effector cells and Fas-deficient target cells. J Immunol. 2003;170:2205-2212.
29. Janka GE, Schneider EM. Modern management of children with hemophagocytic lymphohistiocytosis. Br J Haematol. 2004;124:4-14.
30. Henter JI. Biology and treatment of familial hemophagocytic lymphohistiocytosis: importance of perforin in lymphocyte-mediated cytotoxicity and triggering of apoptosis. Med Pediatr Oncol. 2002; 38:305-309.
31. Moretta L, Moretta A, Hengartner H, et al. On the pathogenesis of perforin defects and related immunodeficiencies. Immunol Today. 2000;21:593-594.
32. Molleran Lee S, Villanueva J, Sumegi J, et al. Characterization of diverse PRF1 mutations leading to decreased natural killer cell activity in North American families with haemophagocytic lymphohistiocytosis. J Med Genet. 2004;41:137-144.
33. Schneider EM, Lorenz I, Walther P, Janka-Schaub GE. Natural killer deficiency: a minor or major factor in the manifestation of hemophagocytic lymphohistiocytosis? J Pediatr Hematol Oncol. 2003;25:680-683.
34. Busiello R, Adriani M, Locatelli F, et al. Atypical features of familial hemophagocytic lymphohistiocytosis. Blood. 2004;103:4610-4612.
35. McCormick J, Flower DR, Strobel S, Wallace DL, Beverley PC, Tchilian EZ. Novel perforin mutation in a patient with hemophagocytic lymphohistiocytosis and CD45 abnormal splicing. Am J Med Genet A. 2003;117:255-260.
36. Katano H, Ali MA, Patera AC, et al. Chronic active Epstein-Barr virus infection associated with mutations in perforin that impair its maturation. Blood. 2003;103:1244-1252.
37. Koch H, Hofmann K, Brose N. Definition of Munc13-homology-domains and characterization of a novel ubiquitously expressed Munc13 isoform. Biochem J. 2000;349(Pt 1):247-253.

Research Report

Central Retinal Artery Doppler Flow Parameters Reflect the Severity of Cerebral Small-Vessel Disease

Masahiko Hiroki, MD, PhD; Kotaro Miyashita, MD, PhD; Hiroshi Yoshida, MD, PhD; Shunsaku Hirai, MD, PhD; Hidenao Fukuyama, MD, PhD

Background and Purpose—We investigated the usefulness of central retinal artery (CRA) Doppler flowmetry in patients with cerebral small-vessel disease (SVD).

Methods—CRA Doppler flowmetry was performed in 103 SVD patients who underwent MRI. Sixty-four adjusted control subjects were also registered. We assessed average CRA flow parameter values for both eyes with the clinical and MRI findings.

Results—Each Doppler flowmetry was performed within 5 minutes. Patients with SVD had significantly lower end-diastolic and mean velocities of the CRA than control subjects; they also had higher pulsatility and resistive indexes. Multivariate analysis showed that the number of small infarcts was an independent predictor of peak systolic and mean velocities. Grade of periventricular hyperintensities was an additional independent predictor of peak systolic and mean velocities, whereas the number of small infarcts was predictive of end-diastolic velocity.

Conclusions—Flow parameters may be useful for the quantitative assessment of SVD severity. (***Stroke.* 2003;34:e92-e94.)**

Key Words: retinal artery ■ small-vessel disease ■ ultrasonography, Doppler

Early and quantitative assessment of small-vessel disease (SVD) is important, but a method has not been established. Recently, we have focused on the central retinal artery (CRA), ≈0.15 to 0.20 mm in diameter distally,[1] which corresponds to a small artery. Because CRA Doppler flowmetry causes minimal discomfort, requires little time, and has high reproducibility,[2] it seems useful for the quantitative assessment of SVD. In this study, we investigated the clinical backgrounds of the CRA flow parameter in patients with SVD confirmed by MRI.

Subjects and Methods

CRA Doppler flowmetry followed carotid ultrasonography in 466 consecutive patients at Tokyo Metropolitan Neurological Hospital between February 2000 and November 2001. We excluded 92 patients who had not had MRI within the year and 58 with ophthalmic disease that affected CRA flow velocity, large-vessel disease, and various therapies. Using Trial of Org 10172 in Acute Stroke Treatment (TOAST) criteria,[3] we selected 103 patients with isolated SVD (mean age, 70.9±9.0 years; 66 men). Furthermore, 64 age- and sex-adjusted controls were selected (the Figure). Informed consent was obtained from all subjects.

Hypertension and high blood pressure were defined by World Health Organization criteria.[4] All clinical background factors except blood pressure and age were assessed as present or absent. Doppler flowmetry was performed by Powervision 6000 (Toshiba Inc, Tokyo) with 5.0-MHz color and pulsed Doppler transducer set at 12.0-kHz pulse frequency and 50-Hz low-cut filter. A 1.0-mm sample volume was positioned in the CRA 3.5 mm below the optic disc. The average value of each flow parameter of both eyes and the common carotid arteries (CCAs) was determined. MRI (1.5-T, Signa Horizon Hispeed, GE) was performed with a spin-echo pulse sequence to generate T1-weighted (repetition time/echo time, 300/8.0 ms) and T2-weighted (repetition time/echo time, 4000/90.0 ms) axial brain images with 6.0-mm slice thickness. On these MR images, lacunar and small white-matter medullary infarcts were defined as small infarcts (<1.5 cm in greatest diameter).[5,6] Periventricular hyperintensities (PVHs) were graded into 3 groups.[7]

Background factors and CRA flow parameters were compared between SVD and control groups with the Mann-Whitney *U* test or χ^2 test. In the SVD group, multiple linear regression analysis of each CRA flow parameter was done for variables with a significant difference or correlation univariately by the Mann-Whitney *U* test, Kruskal-Wallis *H* test, and Spearman's rank correlation test.

Results

Compared with the control group, the SVD group had a significantly higher prevalence of hypertension, smoking, left ventricular hypertrophy, and pulsatility and resistive indexes of CCA and a lower prevalence of end-diastolic and mean velocities of the CCA (Table 1). CRA end-diastolic and mean velocities were significantly lower and CRA pulsatility and resistive indexes were higher in the SVD group than the control group (Table 2).

Received August 5, 2002; final revision received December 5, 2002; accepted December 10, 2002.

From the Human Brain Research Center, Kyoto University Graduate School of Medicine, Kyoto, Japan (M.H., H.F.); Cerebrovascular Division, Department of Medicine, National Cardiovascular Center, Suita, Osaka, Japan (K.M.); and Departments of Neurology (S.H.) Neurophthalmology (H.Y), Tokyo Metropolitan Neurological Hospital, Fuchu, Tokyo, Japan

Correspondence to Masahiko Hiroki, MD, Human Brain Research Center, Kyoto University Graduate School of Medicine, Shogoin, Sakyo-ku, Kyoto 606-8507, Japan. E-mail CYI01752@nifty.ne.jp

Stroke is available at http://www.strokeaha.org

DOI: 10.1161/01.STR.0000075768.91709.E4

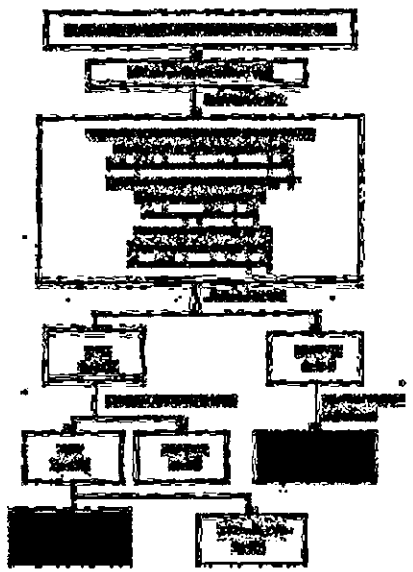

Flow chart showing subject selection. PDF indicates proliferative diabetic retinopathy; CVD, cerebrovascular disease; and LVD, large-vessel disease.

Multiple linear regression analysis showed that the small infarct number was an independent predictor of peak systolic ($B=-0.282$, $P=0.001$) and mean ($B=-0.164$, $P<0.001$) velocities, and CCA resistivity index was predictive of end-diastolic velocity ($B=-2.231$, $P=0.016$) and pulsatility ($B=1.830$, $P<0.001$) and resistivity ($B=0.438$, $P<0.001$) indexes. PVH was an additional independent predictor of peak systolic and mean velocities; small infarct number, of end-diastolic velocity; and age, of pulsatility and resistivity indexes (Table 3).

TABLE 2. CRA Flow Parameters in SVD Patients and Control Subjects

	SVD Patients (n=103)	Control Subjects (n=64)	*P*
Peak systolic velocity, cm/s	8.40±2.64	8.86±2.41	0.159
End-diastolic velocity, cm/s	2.26±0.65	2.63±0.82	0.003
Mean velocity, cm/s	4.57±1.40	5.02±1.31	0.017
Pulsatility index	1.34±0.25	1.25±0.27	0.021
Resistive index	0.72±0.06	0.70±0.07	0.018

Values are expressed as mean±SD. No significant differences were found between left- and right-side values of each flow parameter in SVD and control subjects, respectively.

Discussion

We showed that CRA flow parameters, especially end-diastolic and mean velocities, related to the severity of SVD. It is thought that decreases in these velocities reflect increases in small-artery or arteriolar wall resistance by arteriosclerosis. PVH, lacunar infarct, and small white-matter medullary infarct are pathologically known to be caused by small-artery or arteriolar lesions.[6,8,9] Overall, CRA flow parameters can reflect the grade of PVH and the number of small infarcts. It is reported that carotid atherosclerosis affects CRA end-diastolic velocity,[10] which was related to the CCA resistivity index in our study. Therefore, to assess SVD by ultrasound, both CRA and carotid examinations are necessary. Patients with vascular risk factors such as hypertension often show a

TABLE 1. Subjects' Background

	SVD Patients (n=103)	Control Subjects (n=64)	*P*	OR
Age (mean±SD), y	70.9±9.0	69.7±8.8	0.608	
Male, %	66.0	64.1	0.856	1.09
Hypertension, %	85.4	56.3	<0.0001	4.54
Diabetes mellitus, % (n)	28.4 (102)	17.2	0.099	1.91
Hyperlipidemia, %	40.8	66.7 (60)	0.274	0.34
Smoking, % (n)	64.4 (101)	42.9 (63)	0.005	2.41
Left ventricular hypertrophy, % (n)	61.8 (102)	25.9 (58)	<0.0001	4.63
High blood pressure, % (n)	57.8 (102)	30.1 (60)	0.001	3.20
Calcium antagonist, %	43.7	34.4	0.109	1.48
Angiotensin-converting enzyme inhibitor, %	9.7	9.4	0.530	1.04
CCA flow parameters (mean±SD)				
Peak systolic velocity, cm/s	69.9±16.1	73.7±16.3	0.163	
End-diastolic velocity, cm/s	15.1±5.1	18.9±5.75	<0.0001	
Mean velocity, cm/s	29.7±7.4	33.4±7.4	0.002	
Pulsatility index	1.92±0.54	1.70±0.50	0.002	
Resistive index	0.78±0.07	0.74±0.07	0.004	

OR indicates odds ratio.

TABLE 3. Independent Variables of Each CRA Flow Parameter in SVD by Multiple Linear Regression Analysis

	Variable	B (SE)	P
PSV*	Intercept	9.708 (0.406)	<0.001
	Small infarct	−0.282 (0.084)	0.001
	PVH	−1.497 (0.692)	0.033
EDV†	Intercept	5.688 (0.718)	<0.001
	CCA resistivity index	−2.231 (0.909)	0.016
	Small infarct	−0.070 (0.020)	0.001
MV‡	Intercept	5.319 (0.212)	<0.001
	Small infarct	−0.164 (0.044)	<0.001
	PVH	−0.807 (0.360)	0.027
PI§	Intercept	−0.551 (0.242)	0.012
	CCA resistivity index	1.830 (0.305)	<0.001
	Age	0.006 (0.002)	0.003
RI‖	Intercept	0.252 (0.059)	<0.001
	CCA resistivity index	0.438 (0.074)	<0.001
	Age	0.002 (0.001)	0.001

PSV indicates peak systolic velocity; EDV, end-diastolic velocity; MV, mean velocity; PI, pulsatility index; and RI, resistivity index.

*Adjusted R^2=0.136, F=9.015, P<0.001; †adjusted R^2=0.233, F=11.327, P<0.001; ‡adjusted R^2=0.161, F=10.761, P<0.001; §adjusted R^2=0.380, F=21.670, P<0.001; and ‖adjusted R^2=0.380, F=21.630, P<0.001.

significant reduction in systolic and diastolic CRA velocities,[11] although we did not find these reductions in our subjects. This might be due to organic changes in the small arteries or medical treatment in our subjects.

In conclusion, CRA flow parameters relate to the severity of SVD independently of aging and may be useful as a quantitative indicator. To confirm its clinical application, follow-up study including normal subjects in the community is necessary.

References

1. Richard SS, Michael AL. *Clinical Anatomy of the Eye*. Boston, Mass: Blackwell Scientific Publications; 1996:142–330.
2. Baxter GM, Williamson TH. Color Doppler imaging of the eye: normal ranges, reproducibility, and observer variation. *J Ultrasound Med*. 1995; 14:91–96.
3. Adams HP Jr, Bendixen BH, Kappelle LJ, Biller J, Love BB, Gordon DL, Marsh EE 3rd. Classification of subtype of acute ischemic stroke: definitions for use in a multicenter clinical trial: TOAST: Trial of Org 10172 in Acute Stroke Treatment. *Stroke*. 1993;24:35–41.
4. 1999 World Health Organization-International Society of Hypertension Guidelines for the Management of Hypertension Guidelines Subcommittee. *J Hypertens*. 1999;17:151–183.
5. Special report from the National Institute of Neurological Disorders and Stroke Classification of Cerebrovascular Diseases III. *Stroke*. 1990;21; 637–676.
6. Bogousslavsky J, Regli F. Centrum ovale infarcts: subcortical infarction in the superficial territory of the middle cerebral artery. *Neurology*. 1992;42:1992–1998.
7. Meguro K, Hatazawa J, Yamaguchi T, Itoh M, Matsuzawa T, Ono S, Miyazawa H, Hishinuma T, Yanai K, Sekita Y, Yamada K. Cerebral circulation and oxygen metabolism associated with subclinical periventricular hyperintensity as shown by magnetic resonance imaging. *Ann Neurol*. 1990;28:378–383.
8. Lotz PR, Ballinger WE Jr, Quisling RG. Subcortical arteriosclerotic encephalopathy: CT spectrum and pathologic correlation. *AJR Am J Roentgenol*. 1986;147:1209–1214.
9. Pullicino PM. Pathogenesis of lacunar infarcts and small deep infarcts *Adv Neurol*. 1993;62:125–140.
10. Costa VP, Kuzniec S, Molnar LJ, Cerri GG, Puech-Leao P, Carvalho CA. The effects of carotid endarterectomy on the retrobulbar circulation of patients with severe occlusive carotid artery disease: an investigation by color Doppler imaging. *Ophthalmology*. 1999;106:306–310.
11. Steigerwalt RD Jr., Belcaro GV, Laurora G, Cesarone MR, De Sanctis MT, Incandela L. Ocular and orbital blood flow in patients with essential hypertension treated with trandolapril. *Retina*. 1998;18:539–545.

Decrease in Cortical Benzodiazepine Receptors in Symptomatic Patients With Leukoaraiosis

A Positron Emission Tomography Study

M. Ihara, MD, PhD; H. Tomimoto, MD, PhD; K. Ishizu, MD, PhD; T. Mukai, PhD; H. Yoshida, MD; N. Sawamoto, MD, PhD; M. Inoue, MD; T. Doi, MD; K. Hashikawa, MD, PhD; J. Konishi, MD, PhD; H. Shibasaki, MD, PhD; H. Fukuyama, MD, PhD

Background and Purpose—[^{11}C]flumazenil (FMZ), a ligand that selectively binds to the central benzodiazepine receptor in the neuronal membrane, is useful for evaluating neuronal viability in a positron emission tomography (PET) scan. Using this ligand, we investigated whether there was a correlation between neuronal integrity in various brain structures and dementia in patients with leukoaraiosis.

Methods—Twelve patients with extensive leukoaraiosis on magnetic resonance imaging were divided into groups of patients with or without dementia. Based on a 2-compartment, 2-parameter model that included metabolite-corrected arterial input and PET-measured cerebral radioactivity, the distribution volume of FMZ (FMZ-V_d) was calculated in various regions of interest by nonlinear curve fitting. Additionally, tracer kinetic analysis was applied for voxel-by-voxel quantification of FMZ-V_d, and data analysis was performed by statistical parametric mapping.

Results—The presence of dementia was associated with a reduced FMZ-V_d in widespread areas of the cerebral cortex, including the bilateral frontopolar and frontal/insular areas, the left temporo-occipital border areas, and the left marginal cortical areas.

Conclusions—Differences in neuronal integrity in the cerebral cortex might determine whether patients with leukoaraiosis become symptomatic or not. (***Stroke.*** **2004;35:942-947.)**

Key Words: leukoaraiosis ■ Binswanger's disease ■ receptors, benzodiazepine ■ tomography, emission computed

Vascular dementia develops as a consequence of various types of cerebrovascular diseases, including so-called Binswanger's disease (BD), which might result in a Binswanger type of vascular dementia.[1] Magnetic resonance imaging (MRI) examination of the brain of patients with BD reveals lacunar infarcts in the basal ganglia as well as leukoaraiosis in the periventricular region and centrum semiovale.[1,2] The relation between these findings and the presence of cognitive impairment is still unclear.[1-3] Although some studies reported a link between cognitive impairment and leukoaraiosis in the periventricular white matter,[4] deep white matter,[5] or both,[6] another study found no such link.[7,8] Because MRI is most often used to evaluate leukoaraiosis, inconsistencies between different studies might be attributable to heterogeneity in the underlying pathology of the T2 hyperintensities, which might reflect dilation of the perivascular space, myelin loss, axonal damage, incomplete infarction, or any combination of these.[9]

Another possible explanation for the aforementioned inconsistencies is that cognitive impairment in BD might not be due to the underlying pathology that accounts for leukoaraiosis alone but to the other gray matter lesions that are seen in these patients. Indeed, damage to axons traveling in the white matter also results in damage to their nerve cell bodies in subcortical and cortical gray matter as a result of anterograde or retrograde degeneration.[10] Consistent with this notion was the positron emission tomography (PET) scan finding of a reduction in oxygen metabolism in cortical and subcortical gray matter areas in patients with BD.[11] Another study further suggested that integrity of frontostriatothalamic circuits is pivotal for cognitive function in geriatric patients with leukoaraiosis.[12] Therefore, ischemic lesions responsible for triggering dementia in BD patients might not be confined to the white matter but rather might extend to broader regions, including cortical and subcortical gray matter regions.

In this study, we sought to identify the underlying differences between patients with leukoaraiosis who manifested dementia and those who did not by using the PET scan. As a tracer, we used the central benzodiazepine receptor (cBZR) ligand [^{11}C]flumazenil (FMZ), because coupling of cBZRs to γ-aminobutyric acid type A ($GABA_A$) receptors,[13] which are widely expressed in cerebral cortical neurons,[14] makes FMZ a reliable marker of neuronal integrity.[15,16] We also examined cerebral blood flow (CBF), cerebral metabolic rate of oxygen metabolism ($CMRO_2$), and oxygen extraction fraction (OEF) by using the ^{15}O gas steady-state method in these patients.

Received October 9, 2003; final revision received November 30, 2003; accepted January 8, 2004.

From the Department of Neurology (M.I., H.T., H.S.), the Horizontal Medical Research Organization (M.I.), the Department of Nuclear Medicine and Diagnostic Radiology (K.I., T.M., J.K.), and the Human Brain Research Center (H.Y., N.S., M.I., T.D., K.H., H.S., H.F.), Kyoto University Graduate School of Medicine, Shogoin, Sakyo, Kyoto, Japan; National Institute of Neurological Disorders and Stroke (H.S.), National Institutes of Health, Bethesda, Md.

Correspondence to Masafumi Ihara, MD, PhD. Kyoto University, Horizontal Medical Research Organization, Yoshida-Konoe, Sakyo, Kyoto, 606-8501, Japan. E-mail ihara@kuhp.kyoto-u.ac.jp

Stroke is available at http://www.strokeaha.org

DOI: 10.1161/01.STR.0000122624.32167.e0

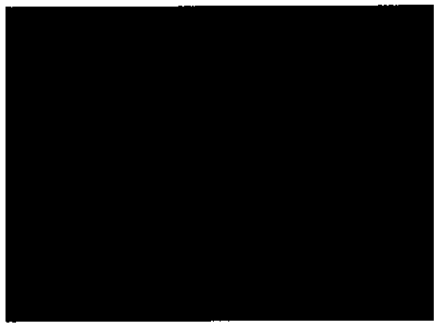

Figure 1. Representative T2-weighted MRIs and summed FMZ images in 2 patients with leukoaraiosis, 1 of whom manifested dementia (A) and the other of whom manifested no dementia (B). Although the MRIs from these 2 patients contain diffuse hyperintensities in the white matter (Schmidt scale 3) and multiple lacunas in the thalamus and basal ganglia, FMZ images show clear contrast in the cortical binding.

Materials and Methods

Subjects

Twelve patients whose T2-weighted MRI scans revealed confluent hyperintensities in the subcortical white matter (Schmidt scale score of 3)[17] and several punctate high-intensity areas in the basal ganglia were studied by PET (Figure 1). They were enrolled in this study because of their MRI-proven neuroradiologic appearances after visiting our Neurology Clinic from May 1999 to March 2002 with various neurologic signs and symptoms. Patients with mild to moderate leukoaraiosis (Schmidt scale score of 1 or 2) were not enrolled in this study to exclude the possibility of leukoaraiosis associated with neurodegenerative disorders such as Alzheimer's disease. Each subject was fully instructed on the experimental procedures and provided written, informed consent, as approved by the Committee of Medical Ethics of our faculty. If the subject was not fully competent due to dementia, we obtained full informed consent from a proxy. None of the patients had apparent lesions in the cerebral cortex or hippocampus. MR angiography or duplex color-coded sonography did not reveal > 50% stenosis in the major intracranial and extracranial vessels. No patient had a history of taking any drugs within the past 3 months that would affect BZR assessment. All subjects underwent a general physical and neurologic examination and neuropsychological assessment, including the Clinical Dementia Rating (CDR)[18] and Mini-Mental State Examination (MMSE). At least 2 neurologists were involved in the neuropsychological assessment independently. If their assessments did not coincide, patients were reexamined by the team for a final verdict.

Synthesis of [^{11}C] FMZ

[^{11}C] FMZ was synthesized as previously described.[19] The radiochemical purity of [^{11}C] FMZ was >99.0%, and the specific activity of the product was 52.5±15.5 GBq/μmol (n=12).

PET Scan

The subjects were scanned with a PET scanner (Advance, General Electric) in 2-dimensional mode for FMZ-PET, as previously reported.[19] Arterial blood samples were drawn, and a metabolite correction of [^{11}C]FMZ was performed by the plasma extraction method.[19] Dynamic imaging was performed in 2-dimensional acquisition mode for 50 minutes after injection (sequence: 6×30 seconds, 7×1 minute, 5×2 minutes, and 6×5 minutes).

All patients except 1 demented woman underwent a ^{15}O gas steady-state study for quantitative CBF and $CMRO_2$ with the same PET scanner. We followed the protocol for inhalation of [^{15}O]CO_2, [^{15}O]O_2, and [^{15}O]CO as previously reported.[20]

Data Analysis

For the analysis of PET images obtained under similar conditions, PET data were reconstructed into 3-dimensional images parallel to the orbitomeatal line, so that each image consisted of 64 planes with 2-mm cubic voxels. Images were displayed by using PMOD software version 2.4 (PMOD Group).[21]

ROI-Based Analysis

Regions of interest (ROIs) were defined on the summed FMZ uptake images by point-and-click or manual drawing mode of PMOD (Figure 2A). Because there are few BZRs in the subcortical regions and none

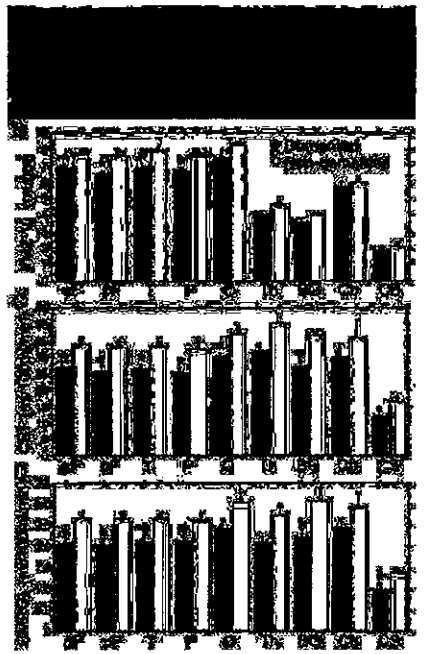

Figure 2. A, ROIs defined on the summed [^{11}C]FMZ uptake image. B–D, Comparisons of FMZ-V_d (B), CBF (C), and $CMRO_2$ (D) in the ROIs between demented (solid bars) and nondemented patients (open bars) with leukoaraiosis. Bars represent SEM. Significant differences ($P<0.05$) between groups are indicated by asterisks. oF indicates orbitfrontal cortex; pF, prefrontal cortex; T, temporal; P, parietal; O, occipital; Th, thalamus; BG, basal ganglia; Cb, cerebellum; and CS, centrum semiovale.

Figure 3. Comparison of regional brain volumetry between demented and nondemented patients with leukoaraiosis. Brain atrophy was assessed on the 3 axial slices; immediately superior to the ventricle (A), through the body of the ventricle (B), and through the anterior and posterior ventricular horns (C). Regions occupied by brain parenchyma, subdural space, and ventricular space are indicated as the ratio to total intracranial area at each level.

in the subdural cerebrospinal fluid space, we could define the cortical mantle, rich in BZRs, by using the differences in FMZ uptake among these regions. For cortical regions, ROIs were defined in the following regions: orbitofrontal cortex, including Brodmann areas 11 and 12; anterior and dorsolateral prefrontal cortex, including areas 9, 10 and 46; temporal cortex, including areas 21, 22, and 37; parietal cortex, including areas 5, 7, 39, and 40; and occipital cortex, including areas 17, 18, and 19, while avoiding intracranial sulci to minimize the partial-volume effect. We also defined ROIs in the thalamus, basal ganglia, cerebellum, and centrum semiovale. ROIs for the centrum semiovale were carefully drawn to prevent contamination by ROIs in the ventricles and gray matter. No ROIs were placed on the periventricular regions because these structures were not easily separable from the ventricles on the FMZ uptake image. Based on a 2-compartment, 2-parameter model with metabolite-corrected arterial input and PET-measured cerebral radioactivity, the distribution volume of FMZ (FMZ-V_d) was calculated in the defined ROIs by nonlinear curve fitting based on the Gauss-Newton method. Values in homologous regions of each hemisphere were averaged. The CO, O_2, and CO_2 images were coregistered to the FMZ image (PMOD software). The ROIs drawn on the FMZ image were transferred to the gas images, and their raw radioactivity counts were measured in all ROIs. Based on the steady-state method, regional CBF, $CMRO_2$, and OEF values were calculated by using each ROI value.[22] The $CMRO_2$ and OEF values were corrected for CBV.[23]

Voxel-by-Voxel Analysis

Using Pmod, pixel-wise calculation was performed to yield parametric images of FMZ-V_d. Briefly, the loaded image data were first pre-processed with arterial input curve. Classic Logan plot model was then applied to the time vector in each individual pixel. The pixel-wise results were assembled into parametric images of FMZ-V_d. These parametric images were analyzed using SPM2 (Wellcome Department of Cognitive Neurology) implemented in Matlab6.5 (The MathWorks Inc). The images were transformed into the standard SPM2 PET template using the early phase of FMZ image added (0 to 10 minutes) as a blood flow image. As a final pre-processing step, the images were smoothed using a 10×10×10 (full width at half maximum) isotropic Gaussian kernel.

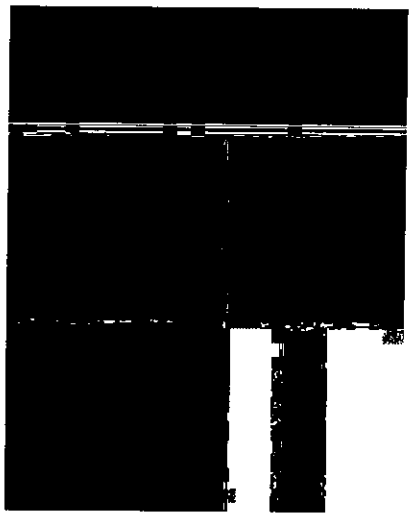

Figure 4. Voxel-based analysis of [^{11}C]FMZ-PET, demonstrating significant decreases in FMZ-V_d in the bilateral frontopolar areas, the bilateral frontal/insular areas, the left temporo-occipital border areas, and the left marginal cortical areas in demented patients ($P_{uncorr}<0.001$). Statistical results are overlaid onto the brain surface (A) and slices (B) of the standard MRI template of SPM2. Color scale: t scores (maximum $t=6.34$, corresponding to $Z=3.78$). R indicates right.

MRI

Brain MRIs were obtained with a 1.5-T MR scanner (Signa Horizon, General Electric). T1-weighted axial images were obtained with a spin-echo pulse sequence with a repetition time of 400 ms and an echo time of 15 ms. Axial T2-weighted images were also obtained (repetition time, 3000 ms; echo time, 100 ms). Axial images were obtained in parallel to the orbitomeatal line. Slice thickness was 5 mm, with an interslice gap of 1.8 mm in the axial plane.

The extent of cerebral atrophy was assessed by regional volumetric measures normalized for total intracranial area on 3 T2-weighted axial slices (see Figures 1 and 3) on a Macintosh PowerPC computer with the use of public domain NIH Image1.61 software (National Institutes of Health, Bethesda, Md). In brief, we manually outlined the inner boundary of the calvarium on T2-weighted axial images to determine the total intracranial area. The images were then binarized with the intensity threshold set at 60% of mean intracranial pixel values within the outlined area. After the ventricular and subdural areas were semiautomatically outlined with the wand tool, the number of pixels in each area was divided by that in the total intracranial area to calculate normalized ventricular and subdural areas. Finally, subtraction of the normalized ventricular and subdural areas from the total intracranial area (value 1.0) yielded normalized parenchymal area.

Statistical Analysis

The statistical significance of intergroup differences was assessed with Fisher's exact test for categorical variables, and the Mann-Whitney U test was used for continuous variables of demographic data and by ANOVA for regional brain volumetry and ROI-based analysis of FMZ-V_d, CBF, $CMRO_2$, and OEF (StatView5.0, SAS Institute).

Demographic Features of the Patients

Variable	Leukoaraiosis With Dementia (BD)	Leukoaraiosis Without Dementia	P
No. of patients	6	6	
Mean age (range), y	76.0±3.7 (69–80)	74.2±4.9 (68–80)	0.48
CDR, (No.)	1 (n=1), 2 (n=3), 3 (n=2)	0 (n=4), 0.5 (n=2)	
Memory (0–3)	2.0±1.0	0.3±0.3	<0.01
Orientation (0–3)	2.0±1.0	0.1±0.2	<0.01
Judgement (0–3)	2.2±0.8	0.3±0.5	<0.01
Community affairs (0–3)	1.9±1.0	0.2±0.3	<0.01
Home and hobbies (0–3)	1.9±1.0	0.3±0.3	<0.01
Personal care (0–3)	1.7±0.8	0.0±0.0	<0.01
MMSE score (0–30)	18.6±3.7	29.0±1.3	<0.01
Orientation (0–10)	6.6±1.8	9.7±0.5	<0.01
Registration (0–3)	2.8±0.4	3.0±0.0	0.30
Attention and calculation (0–5)	2.2±1.6	5.0±0.0	<0.01
Recall (0–3)	1.8±1.1	2.5±0.5	0.30
Language (0–9)	5.6±1.5	8.8±0.4	<0.01
Gait disturbance, No. (%)	5 (83)	2 (33)	0.24
Dysarthria, No. (%)	2 (33)	1 (17)	>0.99
Urinary incontinence, No. (%)	4 (67)	0 (0)	0.06
Hypertension, No. (%)	5 (83)	2 (33)	0.24
BP control (systolic BP >140 mm Hg), No. (%)	1 (17)	0 (0)	>0.99
Diabetes mellitus, No. (%)	1 (17)	1 (17)	>0.99
Cigarette smoking, No. (%)	2 (33)	3 (50)	>0.99
Microalbuminuria, No. (%)	1 (17)	1 (17)	>0.99
Previous cerebrovascular events, No. (%)	2 (33)	1 (17)	>0.99
Previous myocardial infarction, No. (%)	2 (33)	1 (17)	>0.99
Use of antiplatelets, No. (%)	5 (83)	3 (50)	0.55
Use of anticoagulants, No. (%)	1 (17)	1 (17)	>0.99
Total cholesterol, mmol/L	5.72±0.64	5.78±1.06	0.81
Triglyceride, mmol/L	1.51±0.70	1.22±0.58	0.63
Hematocrit, proportion of 1.0	0.37±0.03	0.37±0.03	0.87
Thrombin-antithrombin complex, μg/L	4.0±2.3	2.4±0.4	0.20
Fibrinogen, μmol/L	9.79±1.18	9.38±3.12	0.83
No. of lacunas in the basal ganglia and thalamus	2.5±1.5	2.3±2.1	0.48

Data are presented as mean±SD. BP indicates blood pressure.

For voxel-based analysis, significant differences in FMZ-V_d between groups were estimated according to the general linear model at each and every voxel of the normalized and smoothed images.[24] A linear contrast was used to test the hypotheses for specific focal effects. The resulting set of voxel values for each contrast constituted a statistical parametric map (SPM{t}). The SPM{t} was thresholded at $P_{uncorr}<0.001$ without multiple comparison.

Results

Patient clinical features and demographics are summarized in the Table. Based on their CDR scores, the subjects were divided into 2 groups: demented (group D: CDR of 1, 2, or 3; 1 man, 5 women) and the nondemented (group ND: CDR 0 or 0.5; 3 men, 3 women). There were no significant differences in patient age between the groups. Scores in all 6 cognitive-functional categories of CDR were significantly different between the 2 groups (the Table). Among the 5 cognitive-functional categories of the MMSE, scores in orientation, attention and calculation, and language were significantly different between the groups (the Table). All patients had at least 1 risk factor for ischemic cerebrovascular disease. Although there were no intergroup differences for these categorical variables, neurologic deficits were more frequently found in group D. All 6 demented patients met the criteria of NINDS-AIREN for vascular dementia.[25] The mean±SD number of lacunas in the basal ganglia and thalamus did not differ between the 2 groups.

FMZ-V_d was lower in group D than in group ND in all ROIs (Figure 2B). These reductions reached significance in the orbitofrontal cortex (11.2%), anterior/dorsolateral prefrontal cortex (13.4%), temporal cortex (14.1%), and parietal cortex (13.1%), although significance was not reached in the occipital cortex, thalamus, basal ganglia, cerebellum, and

centrum semiovale. CBF and $CMRO_2$ were also reduced in group D (Figure 2C and 2D). The reduction in CBF reached significance in all cortices examined (orbitofrontal cortex, 20.1%; prefrontal cortex, 21.2%; temporal cortex, 20.7%; parietal cortex, 19.2%; and occipital cortex, 19.6%) as well as in the basal ganglia (26.2%). $CMRO_2$ was significantly reduced in the orbitofrontal cortex (21.3%), anterior/dorsolateral prefrontal cortex (23.5%), temporal cortex (20.3%), parietal cortex (18.2%), basal ganglia (28.1%), and centrum semiovale (29.0%). No significant differences were detected in OEF.

SPM analysis showed that FMZ-V_d was significantly reduced in the bilateral frontopolar areas, the bilateral frontal/insular areas, the left temporo-occipital border areas, and the left marginal cortical areas ($P_{uncorr}<0.001$; Figure 4).

The regional volumetry showed no significant differences in brain parenchymal, ventricular, and subdural areas at the 3 axial levels between D and ND groups (Figure 3). The ventricular space was larger in group D, whereas the subdural space was larger in the ND group.

Discussion

The aforementioned results show that decreases in FMZ-V_d, CBF, and $CMRO_2$ are widespread in the cerebral cortexes in patients with leukoaraiosis who manifest dementia (BD patients) compared with those who do not. Because no significant differences were detected in subdural space between groups D and ND, such difference in FMZ-V_d, CBF, and $CMRO_2$ cannot be attributed to partial-volume effects. FMZ binding reflects neuronal integrity[15,16] and is relatively unaffected by CBF.[26] Our results therefore suggest that neuronal integrity is impaired in BD patients in the cortexes where CBF and oxidative metabolism are also decreased. Although the sex ratio was not completely matched between the 2 groups (there were more women in group D), adjustment for sex would likely have further widened the difference between the 2 groups because FMZ-V_d was reported to be slightly higher in women than in men.[27] In contrast, MRI revealed no significant differences in the parenchymal space, the severity of white matter lesions, or the number of lacunas between demented and nondemented patients with leukoaraiosis. Therefore, neuronal damage that is not visible on conventional MRI might be present in the cerebral cortex and might contribute, at least partially, to the development of dementia.

Leukoaraiosis and fibrohyalinosis of the medullary arteries are predominant in the frontal lobe.[3] In the present SPM analysis, the greatest reductions of FMZ-V_d were seen in the bilateral frontopolar and frontal/insular areas in demented patients with leukoaraiosis. Yao et al[11] and Sabri et al[8] reported that CBF and $CMRO_2$ were significantly reduced not only in the cerebral cortexes but also in the basal ganglia. Because the frontal cortex and the basal ganglia constitute closely connected corticosubcortical circuits through the frontal white matter tracts,[12,28] extensive leukoaraiosis in the frontal white matter might cause circuit disruption and thereby, a loss of executive function and processing speed. Furthermore, frontopolar and frontal/insular areas are postulated to participate in the active maintenance of attention during memory retrieval and other cognitive functions.[29,30] Such top-down control of attention by the frontal cortex might be impaired and therefore contribute to the development of cognitive slowing in patients with leukoaraiosis. Consistent with this notion is that the attention and calculation category of the MMSE was most significantly decreased in demented patients with leukoaraiosis.

Leukoaraiosis seen on T2-weighted images might be due to a variety of different pathologic conditions.[9] In fact, differences in the type and distribution of these lesions might account for differences in neurologic symptoms. Thus, oxidative metabolism in the deep white matter was significantly reduced in demented compared with nondemented patients, suggesting that different pathologies underlie apparently similar T2 hyperintensities in the white matter. More severe white matter damage, such as axonal damage and incomplete infarction, might tend to cause circuit disruption, and such disruption in the circuit connecting frontopolar or frontal/insular areas with subcortical nuclei might lead to neuronal disintegrity as well as dementia. Because conventional MRI cannot differentiate underlying white matter pathologies, functional imaging including FMZ-PET can be an effective premortem modality to detect such circuit disruption. In fact, axonal damage has been reported in autopsied specimens of white matter lesions[31,32] and in demented patients with leukoaraiosis who were examined by ^{1}H MR spectroscopy.[33] Axonal damage can cause retrograde degeneration, which might result in neuronal perikaryal injury and, ultimately, neuronal loss.[10] Indeed, loss of synaptophysin, a neuronal marker, in the cerebral cortex has been reported in the brains of BD patients.[34] Our results are consistent with these findings and further suggest that neuronal injury in the cerebral cortex occurs in BD patients.

In summary, the current study suggests that severe ischemic damage in the white matter can evoke corticosubcortical circuit disruption, possibly leading to impaired top-down control by the frontal cortex. Although a longitudinal study is required to ascertain whether nondemented patients with leukoaraiosis will develop full-blown dementia in the natural course of the disease, therapeutic intervention might be effective to prevent cognitive impairment. Recent evidence suggests promising effects of several acetylcholine esterase inhibitors on symptomatic relief of vascular dementia[35]; however, no definitive therapy has been developed. Therefore, further research is warranted to develop novel strategies to maintain the functional integrity of corticosubcortical circuits.

Acknowledgments

This study was supported by Grants-in-Aid for Scientific Research (B) 14370205 from the Ministry of Education, Culture, Sports Science and Technology and General Research "Grant Science of Mind" and "Aging and Health" from the Ministry of Health, Labour and Welfare to H.F. The authors thank Dr Hideo Saji for his thoughtful review of this manuscript and the staff of the cyclotron unit for their excellent support.

References

1. Pantoni L, Garcia JH. The significance of cerebral white matter abnormalities 100 years after Binswanger's report: a review. *Stroke*. 1995;26:1293–1301.
2. Hachinski VC, Potter P, Merskey H. Leukoaraiosis. *Arch Neurol*. 1987;44:21–23.
3. Hurley RA, Tomimoto H, Akiguchi I, Fisher RE, Taber KH. Binswanger's disease: an ongoing controversy. *J Neuropsychiatry Clin Neurosci*. 2000;12:301–304.
4. De Groot JC, De Leeuw FE, Oudkerk M, Van Gijn J, Hofman A, Jolles J, Breteler MM. Periventricular cerebral white matter lesions predict rate of cognitive decline. *Ann Neurol*. 2002;52:335–341.
5. Leaper SA, Murray AD, Lemmon HA, Staff RT, Deary IJ, Crawford JR, Whalley LJ. Neuropsychologic correlates of brain white matter lesions depicted on MR images: 1921 Aberdeen Birth Cohort. *Radiology*. 2001;221:51–55.
6. Garde E, Mortensen EL, Krabbe K, Rostrup E, Larsson HB. Relation between age-related decline in intelligence and cerebral white-matter hyperintensities in healthy octogenarians: a longitudinal study. *Lancet*. 2000;356:628–634.
7. Schmidt R, Fazekas F, Offenbacher H, Lytwyn H, Bliematl B, Niederkorn K, Horner S, Payer F, Freidl W. Magnetic resonance imaging white matter lesions and cognitive impairment in hypertensive individuals. *Arch Neurol*. 1991;48:417–420.
8. Sabri O, Ringelstein EB, Hellwig D, Schneider R, Schreckenberger M, Kaiser HJ, Mull M, Buell U. Neuropsychological impairment correlates with hypoperfusion and hypometabolism but not with severity of white matter lesions on MRI in patients with cerebral microangiopathy. *Stroke*. 1999;30:556–566.
9. Udaka F, Sawada H, Kameyama M. White matter lesions and dementia: MRI-pathological correlation. *Ann N Y Acad Sci*. 2002;977:411–415.
10. Brodal A, ed. *Neurological Anatomy in Relation to Clinical Medicine*, 3rd ed. New York, NY: Oxford University Press, 1981.
11. Yao H, Sadoshima S, Kuwabara Y, Ichiya Y, Fujishima M. Cerebral blood flow and oxygen metabolism in patients with vascular dementia of the Binswanger type. *Stroke*. 1990;21:1694–1699.
12. O'Brien JT, Wiseman R, Burton EJ, Barber B, Wesnes K, Saxby B, Ford GA. Cognitive associations of subcortical white matter lesions in older people. *Ann N Y Acad Sci*. 2002;977:436–444.
13. Olsen RW. The GABA postsynaptic membrane receptor-ionophore complex: site of action of convulsant and anticonvulsant drugs. *Mol Cell Biochem*. 1981;39:261–279.
14. Fritschy JM, Mohler H. $GABA_A$-receptor heterogeneity in the adult rat brain: differential regional and cellular distribution of seven major subunits. *J Comp Neurol*. 1995;359:154–194.
15. Heiss WD, Grond M, Thiel A, Ghaemi M, Sobesky J, Rudolf J, Bauer B, Wienhard K. Permanent cortical damage detected by flumazenil positron emission tomography in acute stroke. *Stroke*. 1998;29:454–461.
16. Ihara M, Fukuyama H, Lee T, Takao S, Kohara N, Shibasaki H. Delayed synaptic dysfunction of association cortices in carbon monoxide intoxication. *Ann Neurol*. 2001;50:829–830.
17. Schmidt R, Hayn M, Fazekas F, Kapeller P, Esterbauer H. Magnetic resonance imaging white matter hyperintensities in clinically normal elderly individuals: correlations with plasma concentrations of naturally occurring antioxidants. *Stroke*. 1996;27:2043–2047.
18. Morris JC. The Clinical Dementia Rating (CDR): current version and scoring rules. *Neurology*. 1993;43:2412–2414.
19. Magata Y, Mukai T, Ihara M, Nishizawa S, Kitano H, Ishizu K, Saji H, Konishi J. Simple analytical method of ^{11}C-flumazenil metabolite in blood. *J Nucl Med*. 2003;44:417–421.
20. Yamauchi H, Fukuyama H, Nagahama Y, Nishizawa S, Konishi J. Uncoupling of oxygen and glucose metabolism in persistent crossed cerebellar diaschisis. *Stroke*. 1999;30:1424–1428.
21. Mikolajczyk K, Szabatin M, Rudnicki P, Grodzki M, Burger C. A JAVA environment for medical image data analysis: initial application for brain PET quantitation. *Med Inform (Lond)*. 1998;23:207–214.
22. Frackowiak RS, Lenzi GL, Jones T, Heather JD. Quantitative measurement of regional cerebral blood flow and oxygen metabolism in man using ^{15}O and positron emission tomography: theory, procedure, and normal values. *J Comput Assist Tomogr*. 1980;4:727–736.
23. Lammertsma AA, Jones T. Correction for the presence of intravascular oxygen-15 in the steady-state technique for measuring regional oxygen extraction ratio in the brain, 1: description of the method. *J Cereb Blood Flow Metab*. 1983;3:416–424.
24. Friston KJ, Holmes AP, Worsley KJ, Poline JP, Frith CD, Frackowiak RSJ. Statistical parametric maps in functional imaging: a general linear approach. *Hum Brain Map*. 1995;2:189–210.
25. Roman GC, Tatemichi TK, Erkinjuntti T, Cummings JL, Masdeu JC, Garcia JH, Amaducci L, Orgogozo JM, Brun A, Hofman A. Vascular dementia: diagnostic criteria for research studies: report of the NINDS-AIREN International Workshop. *Neurology*. 1993;43:250–260.
26. Holthoff VA, Koeppe RA, Frey KA, Paradise AH, Kuhl DE. Differentiation of radioligand delivery and binding in the brain: validation of a two-compartment model for [^{11}C]flumazenil. *J Cereb Blood Flow Metab*. 1991;11:745–752.
27. Chugani DC, Muzik O, Juhasz C, Janisse JJ, Ager J, Chugani HT. Postnatal maturation of human $GABA_A$ receptors measured with positron emission tomography. *Ann Neurol*. 2001;49:618–626.
28. Alexander GE, Crutcher MD. Functional architecture of basal ganglia circuits: neural substrates of parallel processing. *Trends Neurosci*. 1990;13:266–271.
29. Buckner RL. Functional-anatomic correlates of control processes in memory. *J Neurosci*. 2003;23:3999–4004.
30. Jiang Y, Haxby JV, Martin A, Ungerleider LG, Parasuraman R. Complementary neural mechanisms for tracking items in human working memory. *Science*. 2000;287:643–646.
31. Suenaga T, Ohnishi K, Nishimura M, Nakamura S, Akiguchi I, Kimura J. Bundles of amyloid precursor protein-immunoreactive axons in human cerebrovascular white matter lesions. *Acta Neuropathol (Berl)*. 1994;87:450–455.
32. Akiguchi I, Tomimoto H, Suenaga T, Wakita H, Budka H. Alterations in glia and axons in the brains of Binswanger's disease patients. *Stroke*. 1997;28:1423–1429.
33. Brooks WM, Wesley MH, Kodituwakku PW, Garry PJ, Rosenberg GA. ^{1}H-MRS differentiates white matter hyperintensities in subcortical arteriosclerotic encephalopathy from those in normal elderly. *Stroke*. 1997;28:1940–1943.
34. Zhan SS, Beyreuther K, Schmitt HP. Synaptophysin immunoreactivity of the cortical neuropil in vascular dementia of Binswanger type compared with the dementia of Alzheimer type and nondemented controls. *Dementia*. 1994;5:79–87.
35. Black S, Roman GC, Geldmacher DS, Salloway S, Hecker J, Burns A, Perdomo C, Kumar D, Pratt R, Donepezil 307 Vascular Dementia Study Group. Efficacy and tolerability of donepezil in vascular dementia: positive results of a 24-week, multicenter, international, randomized, placebo-controlled clinical trial. *Stroke*. 2003;34:2323–2330.

Impact of sex and its interaction with age on the management of and outcome for patients with acute myocardial infarction in 4 Japanese hospitals

Kunihiko Matsui, MD, MPH,[a] Tsuguya Fukui, MD, MPH,[a] Kenji Hira, MD,[a] Atsushi Sobashima, MD, MPH,[b] Shuichi Okamatsu, MD,[b] Noriaki Hayashida, MD,[c] Shigemichi Tanaka, MD,[d] and Masakiyo Nobuyoshi, MD[e]
Kyoto, Iizuka, Tokyo, Sapporo, and Kitakyusyu, Japan

Background Several studies from the United States and from European countries have detected sex and age differences in clinical characteristics, management, and outcomes of acute myocardial infarction. The aim of this study was to determine how sex and age influence the management of and outcome for patients with acute myocardial infarction in Japan.

Methods A retrospective cohort study was performed by means of patient chart review at 4 teaching hospitals in Japan. There was a total of 482 patients [136 females [28%], 346 males [72%]] admitted consecutively with a diagnosis of acute myocardial infarction between July, 1995 and June, 1996.

Results Female patients were older and had more comorbid diseases than male patients. Female patients also tended to have more cardiac complications during hospitalization and a greater 30-day mortality [10% vs 4%, $P < .05$]. After adjustment for baseline characteristics and age/sex interaction, it was found that female patients were less likely to undergo thrombolytic therapy, cardiac catheterization, or revascularization, and they had a greater 30-day mortality. These sex differences in cardiac catheterization and revascularization were more pronounced for older patients. On the other hand, the sex differences in 30-day mortality were greater for younger patients.

Conclusions Our data suggest that cardiac catheterization, revascularization and 30-day mortality may have been related to patient sex and age, but further study is needed. [Am Heart J 2002;144:101-7.]

Several studies from the United States and European countries have detected sex differences for clinical characteristics, management, and outcomes of acute myocardial infarction (AMI),[1-25] although some studies suggest there was little to no sex bias in therapy.[26] Generally, female patients are older and less likely to undergo diagnostic and therapeutic procedures than males.[1,2,6,8,10,11,13,17,21]

As for patients in Japan, it has been reported that the management patterns and clinical outcomes of AMI differed according to age brackets.[27] However, it remains to be determined whether there are also sex differences in the management and outcomes of AMI. Because the population in Japan is rapidly graying and has the longest life expectancy in the world,[28] any sex or age differences in clinical management and outcomes will become increasingly significant in the years to come.

Therefore, our aim was to determine how patients' sex and age influence the management and outcomes of AMI in Japan.

From the [a]Department of General Medicine and Clinical Epidemiology, Kyoto University Hospital, Kyoto, [b]Aso Iizuka Hospital, Iizuka, [c]St Luke's International Hospital, Tokyo, [d]Teine Keijinkai Hospital, Sapporo, and [e]Kokura Memorial Hospital, Kitakyusyu, Japan.

Supported by grants from St Luke's Life Science Foundation and Aso Cement Co, Japan.
Submitted March 6, 2001; accepted January 16, 2002.

Reprint requests: Tsuguya Fukui, MD, MPH, Professor of Medicine, Department of General Medicine and Clinical Epidemiology, Kyoto University Hospital, 54 Shogoin Kawahara-cho, Sakyoku, Kyoto 606-8507 Japan.
E-mail: fizt@kuhp.kyoto-u.ac.jp

0002-8703/2002/$35.00 + 0 4/1/123114
doi:10.1067/mhj.2002.123114

Methods

Study sites and population

To meet inclusion criteria for our study, subjects had to be consecutively hospitalized patients with a diagnosis of AMI at 1 of 4 teaching hospitals (Aso Iizuka Hospital, Iizuka; St Luke's International Hospital, Tokyo; Teine Keijinkai Hospital, Sapporo; and Kokura Memorial Hospital, Kitakyusyu) in Japan between July, 1995 and June, 1996. These hospitals, equipped to perform cardiac catheterization and cardiac surgery, were invited to participate in the study through the authors' personal networks. They are therefore not necessarily representative of all hospitals or all teaching hospitals in Japan. Subject patients were identified by reviewing medical records. The diagnosis of acute myocardial infarction was made according to generally accepted criteria, including: (1) a record of elevated creatine kinase (a peak total creatine kinase level exceeding twice the usual upper limit of the reference value used at the individual hospitals, or creatine kinase-MB isoenzyme accounting for ≥5% of the elevated total creatine kinase level), (2) a history of chest pain compatible with myocardial infarction and/or (3) electrocardiogram (EKG) abnormalities defined as 0.1 mV ST-segment elevation in contiguous leads, or 0.1 mV ST-segment depression and/or definite T wave inversion.

Data collection

Detailed chart reviews were carried out by physician reviewers who were not aware of the hypothesis being tested. Variables of interest included sex, age, vital signs (blood pressure and heart rate on admission), transferred status (patients who were brought to the participating hospitals soon after the diagnosis of AMI was made at another hospital but had not received such therapies or interventions as thrombolytic therapy, catheterization, revascularization, or coronary artery bypass grafting [CABG] were included), smoking status, previous cardiac histories (congestive heart failure [CHF], myocardial infarction, angina, revascularization [percutaneous transluminal coronary angioplasty, stent, and other therapies via cardiac catheterization], and CABG), comorbidities (hypertension, diabetes, gastrointestinal disease, liver disease, renal disease, pulmonary disease, and hyperlipidemia), changes in EKG (ST elevation, ST depression), infarct location (anterior, inferior, and other sites), cardiac complications during hospitalization (no complications, recurrent chest pain indicative of ischemia, reinfarction, CHF, pulmonary edema, cardiogenic shock, Mobitz type II block, complete AV block, VF/VT, respiratory failure requiring intubation, cardiac arrest, and death), major procedures (thrombolytic therapy, catheterization, revascularization, and CABG), prescribed drugs (aspirin, β-blocker, angiotensin-converting enzyme [ACE] inhibitor, and calcium antagonist) and length of stay (intensive care unit [ICU], total).

Statistical analysis

The differences analyzed were those in baseline characteristics, management, and outcomes between females and males. The χ^2 test with appropriate degrees of freedom was used to compare categorical variables and the Fisher exact test was employed where appropriate. The student t test was used for continuous variables.

Age and its interaction term with sex were modeled as continuous variables in all multivariate models. This interaction term tested the hypothesis that the association between sex and outcome variables differs according to age. For this purpose, we constructed a series of hierarchic logistic regression models in sequential fashion to evaluate the association of sex with each of the outcome variables, including thrombolytic therapy, cardiac catheterization, revascularization, CABG and 30-day mortality, while controlling for potential confounders. This method of hierarchic modeling allowed us to assess the impact of each of the features added sequentially to the model.[20] On the basis of the results of these logistic regression models, odds ratios of female to male patients were calculated for each procedure and for 30-day mortality from age 60 to 80 by 5-year increments.[29]

We considered association statistically significant at $P < .05$ with 2-tailed distribution.

Results

A total of 482 patients with AMI met the inclusion criteria: 136 (28%) females and 346 (72%) males. Females (average age 70.4 years) were significantly older than males (62.9 years). Patients aged ≥80 years accounted for 13% of females and 6% of males. Females were more likely than males to have histories of CHF (7% vs 1%, $P < .001$), hypertension (54% vs 44%, $P < .05$), and hyperlipidemia (27% vs 14%, $P < .001$), whereas they were less likely to be current smokers (19% vs 60%, $P < .001$) or to have a liver disease (1% vs 5%, $P < .05$). Females had more comorbid diseases than males (1.4% vs 1.2%, $P < .05$), but there were no significant differences in physical findings at the initial presentation, EKG changes, infarct locations, or in time from onset of symptoms to hospital visit (Table I).

The proportion of patients with no cardiac complications during hospitalization was fewer for females than for males (45% vs 60%, $P < .01$). Specifically, females suffered cardiac complications more frequently than males: CHF (26% vs 16%, $P < .05$), pulmonary edema (8% vs 2%, $P < .01$), and cardiogenic shock (21% vs 8%, $P < .001$). The same was true for 30-day mortality (10% vs 4%, $P < .05$) (Table II).

The majority of patients underwent invasive procedures. With respect to sex, females were less likely than males to receive cardiac catheterization (84% vs 95%, $P < .001$) or revascularization (65% vs 76%, $P < .05$). However, there were no sex differences regarding CABG or prescribed drugs. The overall hospital stay was longer for females than males (31.4 days vs 25.1 days, $P < .01$), but not the ICU stay (2.8 days vs 3.2 days, $P < .5$).

The hierarchic models of multivariate analyses were created to estimate odds ratios for undergoing invasive procedures and 30-day mortality after admission for different age groups. The first model included baseline characteristics (sex, age, and the interaction between sex and age). The second model included histories (current smoking status, transferred status, cardiac histories [CHF, angina, myocardial infarction, revascularization, and CABG], and comorbidities) in addition to the variables included in the first model. The third model included, in addition to variables of the second model, initial findings (initial vital signs [heart rate ≥100 beats/min, systolic blood pressure ≤90 mm Hg], EKG changes [ST elevation, ST depression], and infarct location [anterior, inferior]). In these hierarchical analyses for each procedure and 30-day mortality for different age groups, the interaction terms of sex and age were borderline significant in all models of different

	Female (n = 136)	Male (n = 346)	P value for female vs male
History (%)			
Age*	70.4 ± 10.7	62.9 ± 11.6	.0
Referred patient	85 (63)	215 (62)	.941
Current smoker	26 (19)	209 (60)	.001
Previous illness			
CHF	9 (7)	3 (1)	.001
Myocardial infarction	21 (15)	62 (18)	.517
Angina	30 (22)	84 (24)	.606
CABG	2 (1)	3 (1)	.556
Revascularization	6 (4)	40 (12)	.016
Comorbidity (%)			
Hypertension	73 (54)	151 (44)	.047
Diabetes	45 (33)	87 (25)	.078
Gastrointestinal disease	18 (13)	53 (15)	.561
Liver disease	1 (1)	19 (5)	.018
Renal disease	11 (8)	23 (7)	.578
Pulmonary disease	5 (4)	27 (8)	.101
Hyperlipidemia	37 (27)	50 (14)	.001
Number of comorbidities*	1.4 ± 1.0	1.2 ± 1.0	.033
Initial examination			
Heart rate (bpm)*	76.6 ± 22.4	76.7 ± 20.0	.953
Systolic BP (mm Hg)*	128.2 ± 35.6	130.9 ± 29.5	.434
ECG change (%)			
ST elevation	102 (75)	269 (78)	.519
ST depression	41 (30)	89 (26)	.325
Infarct location (%)			
Anterior	55 (40)	140 (40)	.997
Inferior	47 (35)	124 (36)	.792
Other	40 (29)	96 (28)	.715
Time (%)			
Onset of symptoms to visit at hospital (min)†	205 (100, 480)	170 (85, 430)	.954

CHF, Congestive heart failure; CABG, coronary artery bypass grafting; BP, blood pressure; ECG, electrocardiogram.
*Values are mean ± SD.
†Median (25th and 75th percentiles).

age groups for cardiac catheterization ($P < .10$), and significant in all models of different age groups for revascularization ($P < .01$). However, the sex and age interaction terms were not statistically significant for the models covering all age groups for thrombolytic therapy, CABG, and 30-day mortality. Female patients and older patients were less likely to undergo cardiac catheterization and revascularization. Female patients were also less likely to undergo thrombolytic therapy, but the proportion of patients who underwent this therapy was similar for different age groups after adjustment for baseline characteristics, histories, and initial findings. However, in all age groups, there were no significant differences for CABG between sex groups. Thirty-day mortality was significantly greater for female patients, and sex difference tended to be greater in younger age groups. For thrombolytic therapy, cardiac catheterization and revascularization, the changes in the odds ratio among hierarchical models were small, indicating that additional features had little significant confounding effects (Table III).

Discussion

Among the patients with AMI in this study, females were older and sicker than males. After adjustment for the differences in baseline characteristics and age/sex interaction, female patients were found to be less likely to undergo such invasive procedures as thrombolytic therapy, cardiac catheterization and revascularization, and showed a greater 30-day mortality. For cardiac catheterization and revascularization, these trends were more pronounced for older patients. However, the sex difference in 30-day mortality was greater for younger patients.

Our results were consistent with and complemented those of previous studies from other countries. Many studies have demonstrated that sex differences exist in

	Female (n = 136)	Male (n = 346)	P value for female vs male
Complication (%)			
No complications	61 (45)	209 (60)	.002
Recurrent pain	15 (11)	33 (10)	.623
Reinfarction	8 (6)	16 (5)	.568
CHF	35 (26)	55 (16)	.013
Pulmonary edema	11 (8)	8 (2)	.003
Cardiogenic shock	29 (21)	29 (8)	.001
Mobitz type II block	0 (0)	3 (1)	.562
Complete AV block	12 (9)	25 (7)	.553
VF/VT	11 (8)	36 (10)	.44
Respiratory failure	15 (11)	26 (8)	.213
Cardiac arrest	5 (4)	14 (4)	.851
30-day mortality	14 (10)	15 (4)	.013
Therapy (%)			
Thrombolysis	30 (22)	114 (33)	.019
Cardiac catheterization	114 (84)	329 (95)	.001
Revascularization	88 (65)	262 (76)	.015
CABG	10 (7)	15 (4)	.179
Drug (%)			
Aspirin	97 (71)	258 (75)	.467
β-Blocker	14 (10)	21 (6)	.108
ACE inhibitor	53 (39)	134 (39)	.961
Calcium antagonist	77 (57)	221 (64)	.14
Length of stay, days (%)			
ICU *	2.8 ± 4.4	3.2 ± 7.7	.455
Total LOS *	31.4 ± 26.1	25.1 ± 23.4	.01

AV, Atrial-ventricular; VF/VT, ventricular fibrillation/ventricular tachycardia; ACE, angiotensin-converting enzyme; ICU, intensive care unit; LOS, length of stay.
* Values are mean ± SD.

regards to the management of patients with AMI.[1,3,8,10-13,16,17,19-24] Specifically, females are less likely to undergo such invasive cardiac procedures as cardiac catheterization, revascularization, and CABG,[1,8,10,11,15,17,19] and they show greater mortality and morbidity than males.[3,8,11-13,16,20-24]

Our findings showed that the proportion of patients who underwent cardiac catheterization or revascularization was extremely high compared to that reported in other countries,[1,9-11,15,16,19] and the average length of stay was much longer than that in the United States and European countries.[30,31] For example, 84% of the female patients and 95% of the male patients in our study underwent catheterization. Even at these high ratios, multivariate analyses showed that female patients were less likely to undergo invasive procedures such as cardiac catheterization and revascularization, and this phenomenon was more marked among older patients. These results reflect the significance of the interaction term for sex and age in the models for cardiac catheterization and revascularization. One interpretation of these differences is that physicians' decisions for these procedures are influenced not only by the age but also by the sex of patients. The health impact of coronary artery disease among males may be disproportionately emphasized so that the importance of this disease among females may be underestimated.[6] Additionally, elderly patients as a group might not be homogenous enough to make it possible for physicians to reach a clear-cut decision on the basis of the patient's age,[32-34] but it is reasonable to assume that they feel reluctant to perform invasive procedures on elderly patients because an advanced age is regarded as an independent risk factor for cardiac death.[15,35-37] Such considerations may be playing a critical role in physicians' judgments and behaviors. Another possible explanation is that females, especially in Japan, may prefer less aggressive procedures because of their innate and culturally nurtured characteristics.[38] In terms of CABG, however, there was no significant sex difference. In comparison with the results of thrombolytic therapy, cardiac catheterization or revascularization, it could be inferred that CABG has been applied with less bias and more consistent standards. However, these variations of management patterns may have been the result of differences between female and male patients in eligibility for each treatment, as Gan et al suggested.[26]

	Thrombolytic therapy		Cardiac catheterization		Revascularization		CABG		30-day mortality	
	OR	95% CI	OR	95% CI	OR	95% CI	OR	95% CI	OR	95% CI
Age 60 years										
Model 1*	0.78	(0.65-0.93)	1.37	(0.94-2.02)	1.45	(1.18-1.78)	1.57	(1.11-2.22)	1.91	(1.36-2.67)
Model 2†	0.79	(0.66-0.95)	1.42	(0.97-2.08)	1.48	(1.20-1.82)	1.17	(0.81-1.68)	2.36	(1.68-3.32)
Model 3‡	0.71	(0.59-0.87)	1.41	(0.95-2.10)	1.41	(1.14-1.75)	0.73	(0.49-1.09)	1.91	(1.30-2.80)
Age 65 years										
Model 1*	0.73	(0.61-0.88)	0.95	(0.64-1.41)	1.01	(0.81-1.25)	1.45	(1.01-2.07)	1.88	(1.33-2.66)
Model 2†	0.75	(0.62-0.90)	0.96	(0.64-1.42)	1.00	(0.81-1.25)	1.14	(0.78-1.66)	2.19	(1.54-3.12)
Model 3‡	0.71	(0.58-0.87)	0.97	(0.64-1.46)	0.99	(0.79-1.23)	0.79	(0.52-1.20)	1.83	(1.23-2.73)
Age 70 years										
Model 1*	0.68	(0.56-0.83)	0.65	(0.43-0.98)	0.70	(0.56-0.87)	1.34	(0.92-1.93)	1.86	(1.30-2.66)
Model 2†	0.71	(0.59-0.86)	0.64	(0.43-0.97)	0.68	(0.54-0.85)	1.11	(0.75-1.63)	2.04	(1.41-2.94)
Model 3‡	0.71	(0.57-0.87)	0.67	(0.44-1.02)	0.69	(0.55-0.87)	0.86	(0.56-1.32)	1.76	(1.17-2.67)
Age 75 years										
Model 1*	0.64	(0.52-0.78)	0.45	(0.29-0.69)	0.49	(0.39-0.61)	1.23	(0.84-1.81)	1.84	(1.27-2.66)
Model 2†	0.67	(0.55-0.83)	0.43	(0.28-0.66)	0.46	(0.37-0.58)	1.08	(0.72-1.61)	1.89	(1.30-2.76)
Model 3‡	0.70	(0.57-0.87)	0.46	(0.30-0.71)	0.48	(0.38-0.61)	0.93	(0.60-1.46)	1.70	(1.11-2.60)
Age 80 years										
Model 1*	0.59	(0.48-0.73)	0.31	(0.20-0.48)	0.34	(0.27-0.43)	1.13	(0.76-1.69)	1.81	(1.24-2.67)
Model 2†	0.64	(0.52-0.79)	0.29	(0.19-0.45)	0.31	(0.25-0.40)	1.05	(0.69-1.59)	1.76	(1.19-2.60)
Model 3‡	0.70	(0.56-0.87)	0.31	(0.20-0.49)	0.34	(0.26-0.43)	1.01	(0.64-1.61)	1.63	(1.05-2.54)

OR, Odds ratio.
*Adjusted for baseline characteristics (age, sex and the age-sex interaction term).
†Adjusted for baseline characteristics and histories (current smoking status, referred status, previous cardiac histories [CHF, angina, myocardial infarction, revascularization, and CABG], and comorbidities).
‡Adjusted for baseline characteristics, histories, and initial findings [initial vital signs [heart rate ≥100 bpm, systolic blood pressure ≤90 mm Hg], ECG changes [ST elevation, ST depression], and infarct location [anterior, inferior]].

Regarding 30-day mortality, we found the sex difference was greater for younger patients. This finding is similar to the results from previous studies and several hypotheses have been proposed to explain sex differences in mortality.[21,25] For example, greater mortality of female patients might be the result of the underemployment of established invasive procedures and delayed detection of coronary artery disease for females. Nonbiological factors such as behavior, psychologic, and social factors might have something to do with the worse outcomes for females.[25]

However, some contradictory results have been reported with regard to mortality.[4,15,35] Other studies have shown no sex differences in preferences for undergoing invasive cardiac procedures.[39,40] These different results could be due to confounding and interaction with the age of patients.[5,14,20-22,24,25,41-43] Sufficiently large samples and adequate detection and adjustment for interactions with sex and age need to be considered when interpreting the research data. Because each study employed differently designed data collection and analyses procedures, it is difficult to conduct any meta-analysis in this regard.[24] However, recently published large-scale studies showed results similar to ours in that female patients showed greater mortality than male patients among younger age groups after adjustments for the details of important factors including interaction with sex and age.[21,25] Our results also suggest that female patients underwent less aggressive therapy for cardiac catheterization and revascularization. Having undergone these invasive procedures does not necessarily mean having received the best management leading to better outcome,[39] nor can the appropriateness of indications for these procedures be determined with the data at hand. The suspicion thus remains that sex bias for management patterns for these invasive procedures could have affected patients' outcomes.

We also found that the proportions of patients who were taking aspirin (74%) and β-blocker (7%) were fewer than those reported in the United States.[21] An overall look at these findings suggests that the current management patterns for AMI in Japan are somewhat different from the standard practice in western countries. Clinical management is intimately related to the characteristics of a given country's health care system, and although resource-intensive systems typical of countries such as Japan could minimize sex difference in clinical management, an outcome study is necessary to prove whether this is in fact the case.

There are several limitations to this study. First, the sample is relatively small and the subject institutions were not randomly selected. Thus, to what extent our results can be extrapolated to hospitals in general in Japan is not clear. Second, long-term mortality data are not available from our results. However, 30-day mortality figures can help assess at least early outcomes, which reflect disease severity and indicate initial management. Finally, because we obtained all data through medical chart review only, some data for important items were not available. For example, the description of histories and comorbidities depended on individual physicians. Besides, data on ejection fraction, Killip classes, and stress testing (indicators known to be related to disease severity, prognosis and mortality rates) were not included in the current analyses because of the frequent lack of data. However, we used other objective variables in our analytical models, such as age, initial vital signs, and EKG findings.

In conclusion, our results suggest that sex differences may exist in the management of patients with AMI in Japan, and that these sex differences may be greater for older patients. Age was shown to be one of the important independent factors for not undergoing invasive procedures and for high 30-day mortality. Furthermore, patterns of AMI management in Japan seem to be different from those in western countries. By taking into account all the clinical and social factors, the most appropriate management strategies for AMI patients in Japan should be established through an evidence-based approach.

References

1. Krumholz HM, Douglas PS, Lauer MS, et al. Selection of patients for coronary angiography and coronary revascularization early after myocardial infarction: is there evidence for a gender bias? Ann Intern Med 1992;116:785-90.
2. Bickell NA, Pieper KS, Lee KL, et al. Referral patterns for coronary artery disease treatment: gender bias or good clinical judgment? Ann Intern Med 1992;116:791-7.
3. Becker RC, Terrin M, Ross R, et al. Comparison of clinical outcomes for women and men after acute myocardial infarction. Ann Intern Med 1994;120:638-45.
4. Karlson BW, Herlitz J, Hartford M. Prognosis in myocardial infarction in relation to gender. Am Heart J 1994;128:477-83.
5. Yarzebski J, Col N, Pagley P, et al. Gender differences and factors associated with the receipt of thrombolytic therapy in patients with acute myocardial infarction: a community-wide perspective. Am Heart J 1996;131:43-50.
6. Hussain KM, Estrada AQ, Kogan A, et al. Trends in success rate after percutaneous transluminal coronary angioplasty in men and women with coronary artery disease. Am Heart J 1997;134:719-27.
7. Goldberg RJ, O'Donnell C, Yazebski J, et al. Sex differences in symptom presentation associated with acute myocardial infarction: a population-based perspective. Am Heart J 1998;136:189-95.
8. Demirovic J, Blackburn H, McGovern PG, et al. Sex differences in early mortality after acute myocardial infarction (The Minnesota heart survey). Am J Cardiol 1995;75:1096-101.
9. Paul SD, Eagle KM, Guidry U, et al. Do gender-based differences in presentation and management influence predictors of hospitalization costs and length of stay after an acute myocardial infarction? Am J Cardiol 1995;76:1122-5.
10. Schwartz LM, Fisher ES, Tosteson NA, et al. Treatment and health outcomes of women and men in a cohort with coronary artery disease. Arch Intern Med 1997;157:1545-51.
11. Chandra NC, Ziegelstein RC, Rogers WJ, et al. Observations of the treatment of women in the United States with myocardial infarction: a report from the national registry of myocardial infarction-1. Arch Intern Med 1998;158:981-8.
12. Suarez G, Herrera M, Vera A, et al. Prediction on admission of in-hospital mortality in patients older than 70 years with acute myocardial infarction. Chest 1995;108:83-8.
13. Koshs JB, Wilson AC, O'Dowd K, et al. Sex differences in the management and long-term outcome of acute myocardial infarction: a statewide study. Circulation 1994;90:1715-30.
14. Vaccarino V, Krumholz HM, Berkman LF, et al. Sex differences in mortality after myocardial infarction: is there evidence for an increased risk for women? Circulation 1995;91:1661-71.
15. Herman B, Greiser E, Pohlabein H. A sex difference in short-term survival after initial acute myocardial infarction: the MONICA-Bremen acute myocardial infarction register, 1985-1990. Eur Heart J 1997;18:963-70.
16. Marrugat J, Sala J, Masia R, et al. Mortality differences between men and women following first myocardial infarction. JAMA 1998;280:1405-9.
17. Ayanian JZ, Epstein AM. Differences in the use of procedures between women and men hospitalized for coronary heart disease. N Engl J Med 1991;325:221-5.
18. Mark DB, Shaw LK, DeLong ER, et al. Absence of sex bias in the referral of patients for cardiac catheterization. N Engl J Med 1994;330:1101-6.
19. Steingart RM, Packer M, Hamm P, et al. Sex differences in the management of coronary artery disease. N Engl J Med 1991;325:226-30.
20. Vaccarino V, Horwitz RI, Meehan TP, et al. Sex differences in mortality after myocardial infarction: evidence for a sex-age interaction. Arch Intern Med 1998;158:2054-62.
21. Vaccarino V, Parsons L, Every NR, et al. Sex-based differences in early mortality after myocardial infarction. N Engl J Med 1999;341:217-25.
22. Hochman JS, Tamis JE, Thompson TD, et al. Sex, clinical presentation, and outcome in patients with acute coronary syndromes. N Engl J Med 1999;341:226-32.
23. Weaver WD, White HD, Wilcox RG, et al. Comparisons of characteristics and outcomes among women and men with acute myocardial infarction treated with thrombolytic therapy. JAMA 1996;275:777-82.
24. Malacrida R, Genoni M, Maggioni AP, et al. A comparison of the early outcome of acute myocardial infarction in women and men. N Engl J Med 1998;338:8-14.
25. Vaccarino V, Krumholz HM, Yarzebski J, et al. Sex differences in 2-year mortality after hospital discharge for myocardial infarction. Ann Intern Med 2001;134:239-41.
26. Gan SC, Beaver SK, Houck PM, et al. Treatment of acute myocardial infarction and 30-day mortality among women and men. N Engl J Med 2000;343:8-15.
27. Haze K, Oka T, Sumiyoshi T, et al. Acute myocardial infarction